CONSTRUCTION OF A COMPACT, VERSATILE DIODE LASER SPECTROMETER and CHARACTERIZATION OF DYE - SURFACTANT INTERACTIONS

By

Marc Alexander Unger

* * * * * * *

Submitted in partial fufillment
of the requirements for
Honors in the Department of Chemistry

UNION COLLEGE

June, 1993

ABSTRACT

UNGER, MARC A. Construction of a Compact, Versatile Diode Laser Spectrometer *and* Characterization of Dye - Surfactant Interactions. Department of Chemistry, June 1993.

A compact diode laser spectrometer has been designed and built. A diode laser serves as a light source. The sample holder was designed to allow the mounting of optical filters and focusing optics. These optical filters differentiate between transmitted, scattered, and fluorescent light. A photodiode transduces one of these optical signals to a current signal. The electronics were designed to perform current to voltage conversion, amplify the signal, and filter out noise. Further processing and display are performed by a "Virtual Instrument", which is a computer program designed to simulate a physical instrument. Design methodology for the mechanical/optical, electronic, and software aspects of the work is include in the thesis.

The interactions of Methylene Blue (a dye) with itself and with Sodium Dodecyl Sulfate (SDS, a micelle-forming surfactant) have been studied by visible absorption and fluorescence spectroscopy, with fluorescence lifetime techniques, by HNMR and 2D-HNMR spectroscopy, and by reference to the literature. Methylene Blue molecules are found to aggregate by stacking in eclipsed formation. Two effects dominate the interactions between Methylene Blue and Sodium Dodecyl Sulfate below its critical micelle concentration: formation of insoluble MB-DS ion pairs, and solvation of these pairs by 1, 2, or 3 SDS molecules. Hypotheses have been proposed to explain the mechanism of the spectral changes due to dye self-aggregation and aggregation with SDS.

For My Parents

Acknowledgement:

First, I would like to thank all the giants on whose shoulders I am standing.

I would also like to thank Union College for putting so many first-rate minds within my reach. The greatest part of my world view - the greatest part of who I am - has been forged here. In particular I would like to thank the Union College Chemistry Department, for providing the framework and the guidance that helped me develop, not only into a *chemist*, but into a *scientist*, in the broader sense.

Two Professors in particular deserve special mention. Thank you to Professor Werner: It was under his tutelage that I first experienced real research, and it was at his suggestion that I applied for the year abroad at the ETH. Both investments have yielded tremendous returns. Thank you also to Professor Mary Carroll, who pushed me with high expectations, nailed me on my mistakes when it was called for, and contributed immensely to my knowledge of what it is really like to do research.

Thanks as well to Roland Pierson and Joe O'Rourke of the Union College Machine Shop, who did an excellent job of building some difficult (and vital) components, and to Gene Davison of the Union College Electrical Engineering Department, who helped with the electronics.

Marc A Unger

Table of Contents

Table of Figures

Chapter 2

Chapter 3

CHAPTER I:

INTRODUCTION

The work presented here falls into two broad categories. The first is the design, construction, and testing of a compact, versatile diode laser spectrometer with photodiode detectors, capable of absorption, fluorescence, and scattering measurements. The second is the application of this instrument and conventional instruments to study dye-surfactant interactions, in particular those in the Methylene Blue - Sodium Dodecyl Sulfate system.

PART I: THE DIODE LASER SPECTROMETER

Lasers In Spectroscopy

Lasers in general offer a number of very important advantages for use in spectroscopy. The beam of a laser can be focused down to a very small spot size, and thus can illuminate a very small area. This provides the capability for excellent *spatial* resolution. Lasers can also be made to generate very short pulses, and thus can obtain excellent *temporal* resolution. They can also be very highly monochromatic, and thus have very high *spectral* resolution. Because the light generated by a laser is coherent, outgoing photons interfere constructively with one another. Therefore much less of their energy is wasted than in a non-coherent light source, where the photons have random phase

relations to one another, and can interfere destructively with one another.

The effect of all of these traits is to enable us to concentrate energy (photon flux) - in space, in time, and in frequency - on the chemical species of spectroscopic interest. Naturally, the higher the photon flux at a given point, the more photons are available for the chemical species to absorb. For absorbance measurements, a stronger light source means more beam light reaching the detector. At the high end of the concentration range, this means that more light will be available at the detector, giving a greater absolute change in signal for a change in concentration. At the lower end of the concentration range, however, the large light throughput means a *smaller* absolute change in signal for a change in concentration. Thus, in absorbance measurements, a stronger light source shifts the dynamic range of measurement to higher concentrations.

For fluorescence measurements, this increased absorption translates linearly into increased emission, and therefore an increase in sensitivity and a drop in the detection limit. For scattering, an increased photon flux translates linearly into more photons scattered. This is an unequivocal advantage.

Of course, there are also disadvantages to using lasers as light sources for spectroscopy; were there not, laser-based spectrometers would already have taken over the market. There

are three main disadvantages. Lasers are typically much more expensive than lamps. They are also less reliable, and require far more maintenance.[1] Finally, their monochromaticity is not always an advantage: Lasers are not generally tunable. With the exception of the dye laser, they operate at only one wavelength or a few different wavelengths.

Diode Lasers

Diode lasers have significant advantages over more conventional lasers. Diode lasers can be thought of as light emitting diodes (LEDs) with mirrored sides. As in a normal pn-junction diode, current flows when the applied voltage pushes electrons and holes toward the pn junction, where the electrons fall into the holes, annihilating the pair. In an LED, the energy difference between separated electrons and hole is enough to cause emission of a photon in the visible wavelengths. In a diode *laser*, the pn junction serves as the laser medium; the surfaces of the junction are mirrored to form a Fabry - Perot resonator[2]. One side is fully reflective, and the opposite side only partially reflective, in order to allow the beam to escape. The diode laser is, then, a solid state device, and it derives its advantages over other types of lasers from this fact. Solid state devices are as a rule very reliable, fairly inexpensive, and small; Therefore, two of the three major disadvantages of lasers in spectroscopy do not apply to diode lasers: they are not expensive, and they are not unreliable.

Diode lasers can have small spectral linewidths (down to ten MHz - one part in 10^8 - with proper controls). Power consumption is also low[1] - the laser dealt with in this work, for instance, will run for six hours (or more) on a nine-volt battery. As a result of this low power consumption, they can be driven directly by very simple electronic circuits, without the need for large, high-voltage power supplies as are common for many conventional lasers. Their response times are also reasonably fast; the model dealt with here has a rise time of approximately five ns.

There are some disadvantages, also. Diode lasers have relatively low power outputs compared to other types of lasers. (However, according to a recent review article[1], the maximum power available approximately doubles every year.) Diode lasers which lase in the red region of the visible spectrum and far into the IR region are readily available for purchase. As this project began, the lower limit on wavelength for commercially available diode lasers was about 640 nm; it was difficult to attain the high differences in electron and hole energies necessary to produce shorter wavelength photons due to the nature of the semiconductor pn junction. The author of a review article current at that time had predicted an improvement of about ten nm per year.[1] Recently, laser diode was constructed that lases in the blue-green region of the spectrum,[3] thus outstripping the reviewers prediction of improvement by about a factor of 100.

The work in this paper was carried out with the (commercially available) red-lasing diode lasers. Despite their wavelength limitations, laser diodes clearly outperform conventional lasers with respect to two of the three major laser limitations: cost and reliability. This was enough to motivate the construction of a diode laser spectrometer.

It would be helpful to have access to the entire visible spectrum. Only a small number of compounds fluoresce following absorption in the red end of the visible spectrum. This limits the number of compounds that can be detected using the spectrometer. The wider wavelength range promised by the blue-green laser diode will allow much more general application. However, the fact that few compounds fluoresce at the red end of the visible spectrum also implies that there are very few compounds that will fluoresce and *interfere* with the fluorescence of the desired species.[1] This lack of interference has been exploited to construct diode laser systems with extraordinary sensitivity. Johnson *et al.* were able to attain a detection limit as low as 47,000 molecules with one such system.[4]

Photodiode Detectors

Photodiode detectors also offer advantages over more conventional detectors. Photodiode detectors perform essentially the reverse function of light emitting diodes; whereas LEDs produce photons when electrons fall into holes across a pn

junction, photodiodes absorb photons at the pn junction to split "neutral" atoms into electron - hole pairs.[5] The resultant current is proportional to the amount of light striking the photodiode. Photodiodes, too, are solid state devices. As stated before, solid state devices are very reliable, fairly inexpensive, and small - particularly in comparison to other detectors, such as photomultiplier tubes or charge-coupled devices. The sensitivity of a photodiode detector is not as high as that of a photomultiplier tube; however, its linear dynamic range is very large. The intensity of the laser yields more signal than a conventional light source, thus tending to offset the relative lack of sensitivity of the detector. Furthermore, because the detector is solid state, it can be interfaced easily to simple electronic circuits.

The entire instrument is solid state (with the possible exception of a monochromator, which may be added later). Our instrument is small, inexpensive, and reliable. Furthermore, it is easily minaturizeable, and has very low power consumption. This opens up the possibility of a portable - even handheld - spectrometer, for use in the field. Because all the components are solid state, it is *possible* to put a laser diode, sample "well", photodiode detectors, and electronics on a small stack of silicon chips. Present work limits itself to a macroscopic instrument.

PART II: DYE - SURFACTANT INTERACTIONS

The Methylene Blue - Sodium Dodecyl Sulfate chemical system was chosen for study for a number of reasons. First, a test substance for the diode laser spectrometer was needed - preferably one which allowed absorbance, fluorescence, and scattering measurements. As mentioned previously, there are few compounds which fluoresce at the longer-wavelength end of the spectrum. Methylene Blue, a strongly red-absorbing dye molecule, is one of them.[1] Sodium Dodecyl Sulfate, a micelle-forming surfactant, is a good light scatterer, but does not absorb or fluoresce significantly. The two molecules can therefore be used as benchmarks, for comparison of the laser diode instrument to conventional instruments.

The two molecules also have other uses. Methylene Blue is often employed as a marker for biomolecules.[6] SDS is used to solubilize biomolecules in (for instance) gel electrophoresis.[7] Both of these uses depend on the fact that the molecules are amphiphilic - they have both hydro*philic* and hydro*phobic* character, as do the vast majority of biomolecules. Driven by the hydrophobic effect, these amphiphilic molecules aggregate with one another in such a way as so bring the hydrophilic moieties to the surface of the aggregate (where they can interact with water) and the hydrophobic moieties to the interior (where they are more shielded from water). In the case of dyes, this leads to the formation of rather amorphous aggregates. In the case of

surfactants, the molecules cluster together to form a semi-spherical micelle, with polar heads sticking out into the polar solvent and hydrocarbon tails clustered in the micelle interior.[8] In the case of proteins, the hydrophobic effect plays a strong role in the correct folding of the protein.[9,10]

As one might expect, dyes and surfactants, being both amphiphilic, form complexes with one another.[8] The aggregation of the dye molecules with the surfactants (as well as with other dye molecules) causes changes in the optical spectra of the dyes; These spectral changes, as well as information obtained with other characterization techniques, provide information on the nature of the dye-surfactant interactions, which are not well understood at present. Since the presence of both hydrophilic and hydrophobic moieties in the same molecule is truly pervasive in biology, the field is obviously of some general interest. If dye-surfactant interactions can be understood and characterized, dye molecules can be used as probes of *surfactant - surfactant* interactions, with a possible generalization to study of the ubiquitous and extremely important hydrophobic effect. The problem of dye-surfactant interactions is also a challenging interesting puzzle in its own right.

LITERATURE CITED

1. Imasaka, T.; Ishibashi, N. *Anal. Chem.* **1990**, *62*, 363A.

2. Mionni, P.; Eberly, J. *Lasers;* Wiley: New York, 1988

3. Neumark, G.; Park, R.; DePuydt, J. *APS News.* **1993**, *2(3)*, 34-36.

4. Johnson, P. *et al., Anal. Chem.* **1989**,*61*, 861-863

5. Skoog, D. *Instrumental Analysis,3rd Ed.*; Saunders: New York, 1985, p 140.

6. Haugland, R. *Molecular Probes;* Molecular Probes Inc.: Eugene, 1992.

7. Stryer, L. *Biochemistry*; Freeman: New York, 1988

8. Diaz Garcia, M.; Sanz-Medel A.; *Talanta*, **1986**,*33*, 255

9. Tanford, C. *The Hydrophobic Effect;* Wiley: New York, 1973, Introduction.

10. Creighton, *T. Proteins;* Freeman: New York, 1984.

CHAPTER II:

THE DIODE LASER SPECTROMETER

OBJECTIVES AND OVERVIEW

The primary objective of this research was to create a compact diode laser spectrometer capable of measuring absorption, fluorescence, and scattering. The design methodology, construction, and testing of the completed instrument are described in this section.

In general, any analytical system must perform certain basic steps in order to obtain useful information from a physical system. These steps are:

Selection of desired signal
Detection (signal transduction)
Amplification
Purification
Processing
Readout

In the case of this diode laser spectrometer, the physical events which we want to observe - absorbance, fluorescence, and scattering - are generated by shining the beam of a visible semiconductor laser through our sample. Figure 2-1 shows a Jablonski energy level diagram of these processes. By means of lenses, filters, and/or a monochromator, we select the signal that we want - absorbance, fluorescence, or scattering - and separate it from the unwanted signals. The photodiode transduces the

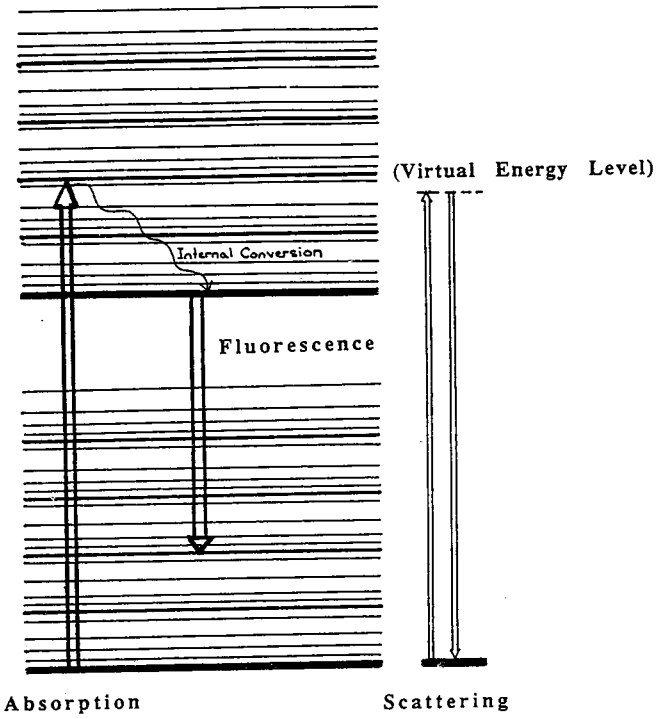

Jablonski Diagram

Figure 2-1

desired optical signal to an electronic one; incident light creates a current of electrons. The electrical circuit amplifies the signal and removes noise. Finally, computer hardware and software processes the data and displays it in useful fashion.

CONSTRUCTION

The design and construction of the instrument can be divided logically into four areas: the laser module, the sample holder (encompassing the mechanical and optical aspects of the design), the electronics (comprising signal transduction and electronic manipulation), and the computer (data acquisition, manipulation, and readout). The three areas of development have been separated here for purposes of clarity, but proceeded simultaneously in the real world.

The Laser Module:

Laser packages were purchased from Power Technology Inc. These packages, cylinders 0.5 by 2 inches long, contained not only the laser diodes, but also adjustable focusing/collimating optics and stabilization electronics. In order to avoid power surges, noise, and transients, 6 V lantern batteries were used to power the lasers.

The laser was electrically isolated, held in place, and kept at a steady temperature by mounting it in a plastic sleeve in an

aluminum block. As the alignment of the laser proved to be critical for absorption measurements, a new laser mount was designed, which could be firmly attached to both the sample holder (described below) and the optical bench. See Figure 2-2.

The Sample Holder:

The sample holder was designed with one input channel and three output channels, with the sample cell at the junction. The sample holder design is shown in Figure 2-3. Laser light is admitted through the input channel to the sample cell, where it may be absorbed or scattered.

Signal Differentiation

The light which is transmitted through the cell passes into the 180° channel, where it can be detected. Since the ratio of light transmitted through the sample (I) to light transmitted through a reference blank (I_O) can be related to the absorbance by

$$A = abc = - \log(I/I_O),$$

the 180° channel is called the absorbance channel. (A = Absorbance, a = molar absorptivity, b = path length, c = concentration.)

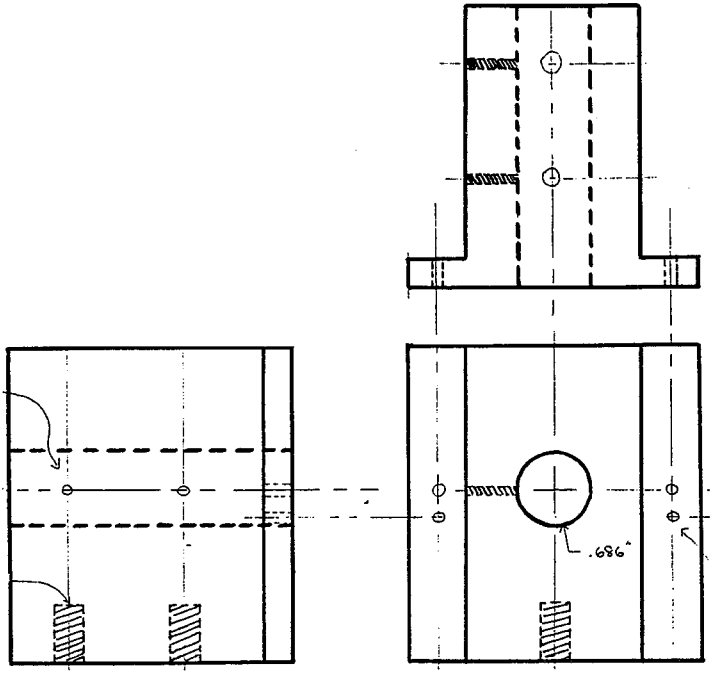

Laser Mount

Figure 2-2

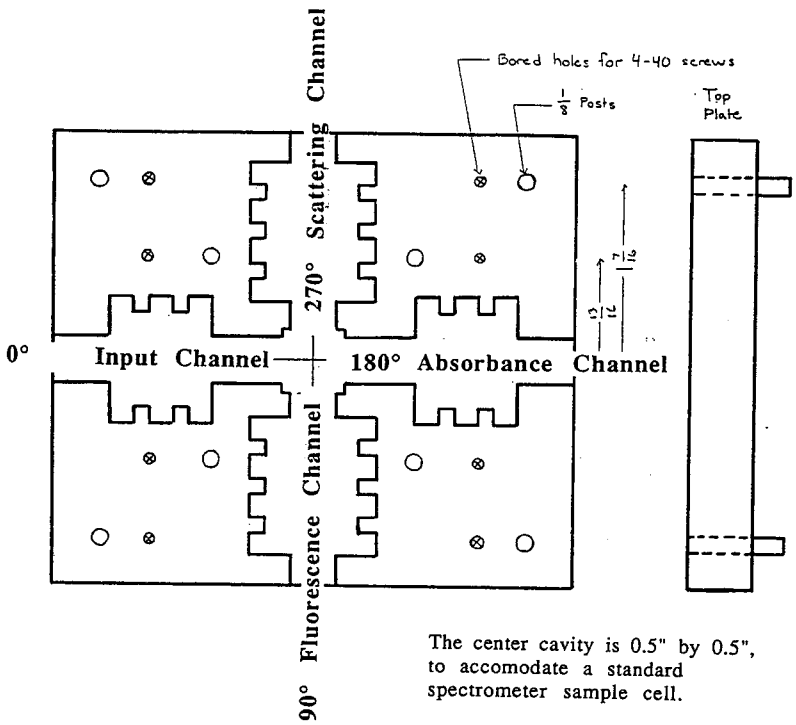

Sample Holder

Figure 2-3

It is important to note that all three processes - absorption, fluorescence, and scattering - are taking place simultaneously. The physical properties of these events must be used to differentiate them. Obviously, transmittance occurs only in a straight line. Scattering due to particles much smaller than the wavelength of light (Rayleigh scattering) occurs according to

$$I = I_o c M g(\theta), \text{ where}$$
$$g(\theta) = 1 + \cos^2\theta \text{ for unpolarized light, or}$$
$$= \sin^2\theta \text{ for polarized light} \quad .$$

(I = scattering intensity at angle θ, I_o = the incident intensity, c = the solute concentration, M = its molar mass, and A = a constant.)[1] Figure 2-4 shows the angular dependence of scattering intensity. Fluorescence occurs randomly in all directions.

In this case, we do not need to differentiate between the three types very carefully for our absorption measurement. Because we are using a laser as a light source, our transmitted beam should be very intense. Because fluorescence occurs randomly in all directions, the amount of fluorescence and scattering that reaches the detector will be proportional to the fraction of surface area that the detector surface takes up on a sphere:

$$F = F_o (A_{det}/A_{susp})$$
$$= F_o (A_{det}/4\pi r^2)$$

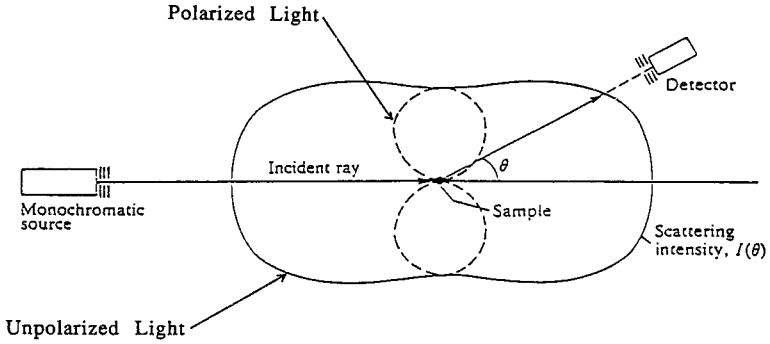

Adapted from Atkins, *Physical Chemistry*, p 694

Rayleigh Scattering

Figure 2-4

(A_{det} = detector area, F = detected fluorescence, F_o = fluorescence yield, A_{susp} = surface area of sphere, r = radius of sphere) Because our detectors are very small (1 mm^2 or less), not much fluorescence will arrive at the detector. (Example: Assuming a point source, for r = 20 mm, $F_{det} = 0.0018\ F_o$.) Furthermore, if the absorbance is higher than 0.1 (i.e. if $I/I_o < 10^{-0.1} = 0.79$), then our yield of fluorescence for a given incoming light intensity will decrease due to self-quenching and self-absorption.[2] Finally, we are using a laser as a light source, and laser light is plane polarized; therefore, from the Rayleigh scattering formula above, there will be no scattering intensity in the forward direction. Therefore, for all practical intents and purposes, fluorescence and scattering will be negligible compared to transmitted light at our absorption detector.

From this analysis, we can also see that it is desirable to minimize the distance between the sample and the fluorescence and scattering detectors, and (if possible) to increase the detector area. In fact, inserting a lens in the channel close to the sample, in such a fashion as to focus collected light on the detector, accomplishes both of these ends. The relevant r is then the distance to the lens, and the relevant A is the area of the lens; In this fashion we can increase the scattering and fluorescence light intensity at the detector substantially, as will be derived below.

In the channels at 90° to the input channel, light from both fluorescence and scattering is present. To differentiate the fluorescence and scattering signals we rely on another physical difference in the signals. Scattered light is inherently the same wavelength as the light source. The energy of a photon produced by fluorescence will be lower than that of a source photon because of the Stokes shift. (See the Jablonski diagram of Figure 2-1) Therefore, the wavelength of fluorescent lig will be longer than the wavelength of the light source. For the scattering channel (which will be arbitrarily called the 270° channel), a line filter which passes only a narrow band of wavelengths centered at the laser wavelength will eliminate the vast majority of the fluorescence signal. (See Figure 2-9.) In order to be certain that the incoming laser beam is sufficiently monochromatic, we can use an identical line filter in the input channel. For the fluorescence channel (arbitrarily called the 90° channel), a cutoff filter which blocks the laser wavelength but passes wavelengths which are longer will eliminate the scattering signal. Alternately, a monochromator could be employed; this has the advantage of allowing true wavelength selectivity, rather than detecting a wide range of fluorescence wavelengths simultaneously. However, it also has the disadvantage of being rather large in comparison with the rest of the instrument.

It is because the signals can be differentiated that the sample holder was designed with one input channel and three output channels: an absorbance channel in straight-line geometry

to the input channel, and fluorescence and scattering channels, each at 90° to the input channel. From the analysis above, it should be clear that we also need to be able to mount lenses and filters in the channels. In addition, we must allow for mounting the photodiode detectors (in order to assure a stable alignment) and for blocking room light (in order to avoid extraneous signals at the detectors.

Optics

All of these considerations were satisfied by designing slots in the input and output channels. The slots hold tight-fitting metal slats. The unmodified slats block room light. By relatively simple machining, it is possible to mount lenses, filters, and the photodiodes themselves in the slats. (See Figure 2-5.)

The question then became one of where to put the slots. There were several constraints on placement. The first and most obvious was the mechanical constraint: there must be enough metal to hold the sample cell and slats in place, and the sample holder must remain physically durable. It must be possible to mount the lenses and filters in the slats, or in the slots themselves. A second set of constraints stems from optical requirements; these constraints will be dealt with presently. Finally, it was essential that the final design could be built by the Union College machine shop with available tools.

Photodiode Mounting Slat

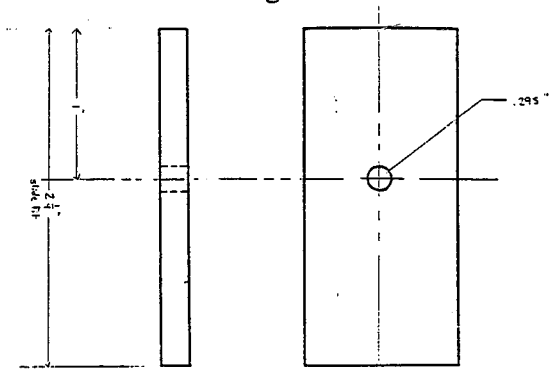

15 mm Lens Mounting Slat

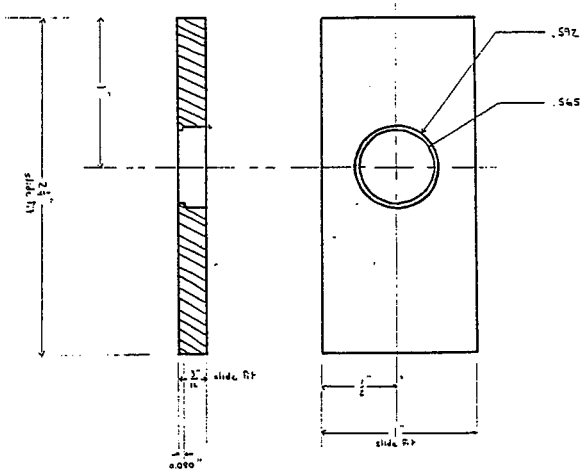

Figure 2-5

The constraints arising out of optical requirements were by far the most difficult to satisfy. The placement of the slots in the fluorescence/scattering channels would be consistent, in an optimal case, with both direct focusing by a lens onto a photodiode detector and coupling to a monochromator before a detector. It will be shown that these two functions require very different lens configurations.

Direct focusing

We will consider the situation where the laser beam, the lens axis, and the detector are in one plane; this is easily accomplished experimentally. The laser beam passes through the sample cell, illuminating a 10 mm path. Given that the light will radiate in all directions, the question is: how much of it will be focused on the detector? We consider two cases (See Figure 2-6 a and b):

Case I. the 2f/2f case. The laser beam and the detector are both twice the lens' focal length from the lens. In this configuration, the image at -2f is simply inverted at 2f. If our detector is 1 mm wide, only 1 mm of the illuminated beam - 1/10 of the light projected on the lens - will project onto the detector. Multiplying by the fraction of the total fluorescence that will be projected on the lens (the surface area of the lens/the surface area of a sphere of radius 2f):

$$I_{det} = (1/10)(\pi r^2)/\{4\pi(2f)^2\} = r^2/(160\ f^2).$$

a. 2f/2f configuration

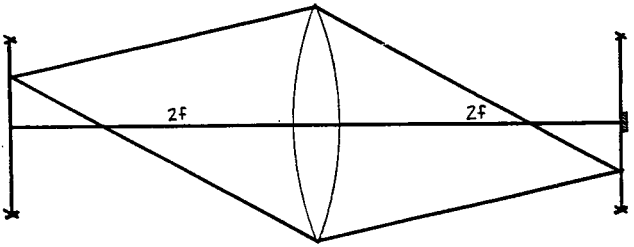

Beam through sample cell

Image of Beam

b. f/f configuration

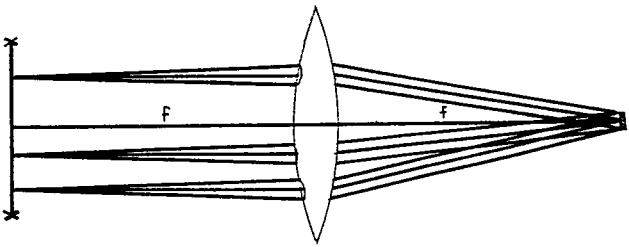

Top View; Beam, lens, and detector are coplanar

Direct Focusing

Figure 2-6

Case II. the f/f case. The laser beam and the detector are both the lens' focal length from the lens. By definition, a lens of focal length f focuses parallel rays to a point at distance f. In this case, we are considering primarily the fluorescence radiated parallel to the lens axis. Since the detector is 1 mm wide, we impose the reasonable assumption that a ray will make it to the detector if it is within 0.5 mm of being parallel when it comes to the lens. We then calculate the fraction of fluorescence from one point in the laser beam that will be projected on the 0.5 mm radius "target" on the lens (the target area / surface area of a sphere of radius f), and note that this will be the fraction of *each* point in the illuminated beam, and therefore the fraction of the total fluorescence intensity:

$$I_{det} = \{\pi(0.5)^2\}/\{4\pi(f)^2\} = 1/(16\ f^2).$$

(Obviously, if the diameter of the lens is less than 10 mm, I_{det} will decrease in direct proportion.)

If we choose r = 5, we can see that the 2f/2f configuration will collect 2.5 times as much light as the f/f configuration. However, in the interests of compactness, the f/f configuration is far superior, as it takes up only 1/4 as much space. Moreover, as the size of the lenses shrinks below 10 mm in diameter, $I_{det,2f/2f}$

shrinks as r^2, whereas I_{det}, f/f shrinks only as r. Thus, the f/f configuration is superior for compactness and miniaturization potential. So for focusing to a spot with a single lens, we want

$$p = q = f.$$

f-matching

With the monochromator, we must "f-match" the entrance optics to the monochromator. In simple terms, we must control the steepness of the cone of light incident upon the monochromator entrance slits. If we do not do this, we may underfill or overfill the diffraction grating in the monochromator; the penalty would be loss of resolution or excessive stray/scattered light in the monochromator, neither of which are acceptable. Figure 2-7 shows the effects of underfilled, filled, and overfilled gratings.

f-number is defined as the ratio of the equivalent focal length of a lens to the diameter of its entrance pupil.[3] For our purposes, the entrance pupil will be the diameter of the lens open to transmit light; in optics terminology, this is the *aperture stop*. (See Figure 2-8)

The following procedure was developed by the author to aid selection of slot distances for the sample holder. Given the focal length f and aperture stop AS of the lens, and the required

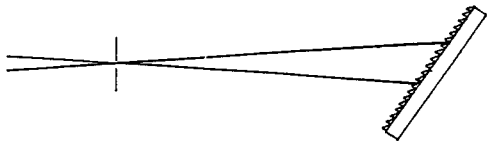

Underfilled Grating:
Incoming light is focused on a small area of the grating, leading to poor resolution.

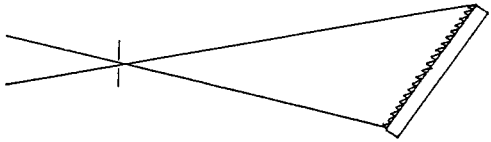

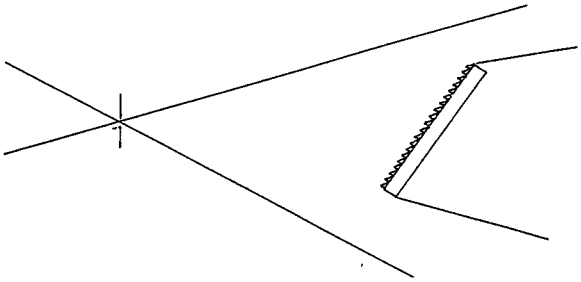

Overfilled Grating:
Part of incoming light misses the grating, leading to reduced signal intensity and large amounts of stray light in the monochromator.

Underfilled, Filled, and Overfilled Gratings

Figure 2-7

To understand how a complete monochromator system is characterized, it is necessary to start at the transfer optics that brings light from the source to illuminate the entrance slit. (See Fig. 12). Here we have "unrolled" the system and drawn it in a linear fashion.

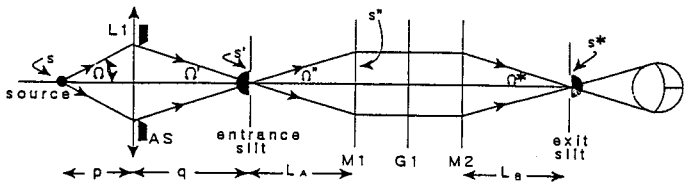

Figure 12 - Typical Monochromator System

AS - aperture stop
L1 - lens 1
M1 - mirror 1
M2 - mirror 2
G1 - grating
p - object distance to lens L1
q - image distance from lens L1
F - focal length of lens L1 (focus of an object at infinity)
d - the clear aperture of the lens (L1 in diagram)
Ω - half-angle
s - area of the source
s' - area of the image of the source

Adapted from Lerner, *The Optics of Spectroscopy*, pp 14-15

Figure 2-8

f/number, this procedure determines the necessary object distance p (the sample - slot distance) and the relative image size at the monochromator entrance slit.

1. given AS, use $f/\# = q/AS$ to find q, the image distance.
2. given q and f, use $1/f = 1/p + 1/q$ to find p
3. given p and q, use $m = q/p$ to find the magnification m

Obviously, the greater the magnification, the less concentrated the light at the monochromator slits, and the weaker the observed signal.

By comparing a relatively large number of commercially available lenses' focal lengths and diameters and determining the necessary p's for their use, comparing those p's with those necessary to do simple focusing to a spot ($p = q = f$), and choosing the p values that made for a mechanically realizable design, a good set of slot distances was achieved. Table 2-1 lists the object (p) and image (q) distances that are easily available from the slot distances of the sample holder.

In addition to the above considerations, it was also necessary to make the sample holder light tight, and to provide for it to be mounted on an optical bench, and for other components to be firmly attached to it. The resulting design is the one shown in Figure 2-3. The sample holder with the filters necessary to differentiate the optical signals is shown in Figure 2-9.

Table 2-1

Available Object and Image Distances in the Sample Holder

Fluorescence Channels

Slot	p	q's
1	12-17	7-11, 15-19, 23-27, (33)
2	21-25	7-11, 15-19, (25)
3	28-33	7-11, (17)
4	36-40	(9)

Absorbance Channels

Slot	p	q's
1	21-25	7-11, 15-19, (30)
2	29-33	7-11, (22)
3	37-41	(15)

p is the object distance in mm; *q* is the image distance in mm. Parentheses indicate mounting on the exterior of the sample holder.

Sample Lens Uses

Lens	Diam	f	f-match slot	f/f slot
32014	12	12	1	1
32013	12	18	3	1
32011	12	24	-	2
32003	15	30	-	-

Diam is the diameter in mm; *f* is the focal length in mm. *f-match slot* is the slot appropriate for f-matching to the monochromator; *f/f slot* is the slot appropriate for direct focusing.

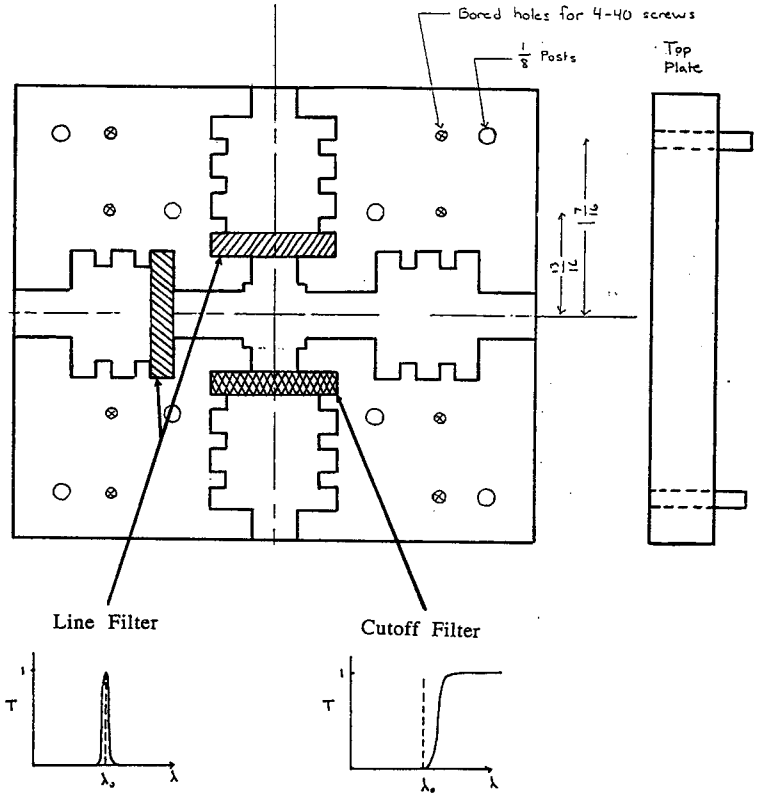

Sample Holder with Filters

Figure 2-9

The Electronics

The selection of the desired optical signal has been accomplished by the sample holder. The electronics in turn perform signal transduction, amplification, and purification.

The strategy behind the design and construction of the electronics was to begin with a circuit intended for steady-state measurements under manual control, later progress towards circuitry that could be controlled by a computer, and eventually move towards a circuit capable of making time-resolved measurements on the order of a few nanoseconds. The design was intended to be modular, and to make use of circuits from electronics literature as much as possible. At present, we have advanced to the second stage; the offset can now be controlled from the computer. Note that further processing of the data and display of the information are performed by the computer.

First Generation Circuit

The first step in the creation of the detector electronics was to choose a current-to-voltage conversion circuit. The photodiode manufacturer's testing circuit is shown in Figure 2-10. This circuit employs a biasing voltage, which increases current by attracting electrons to the cathode and repelling holes toward the anode. Although this increases signal, it also increases dark current (and

Fig. 2 – SWITCHING TIME TEST CIRCUIT

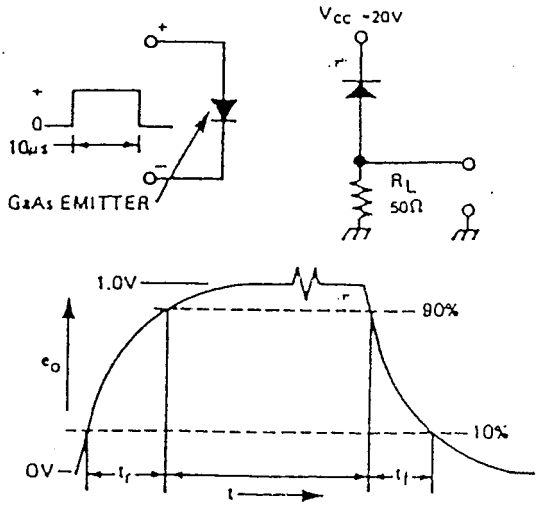

Manufacturer's Testing Circuit

Figure 2-10

noise) substantially. According to manufacturer specifications, dark current with a 20 V bias is 2 x 10^{-8} A; measurements made with no bias voltage place an *upper limit* on dark current of 6 x 10^{-11} A. Preliminary tests also showed that the manufacturer's circuit was difficult to interface with op-amp-based circuitry, and the higher voltages required to bias the photodiode would complicate the electronics. Therefore, this circuit was rejected in favor of the simple op-amp based circuit shown in Figure 2-11, which was designed by the author based on component circuits from the literature.[4,5]

This circuit was designed in modules. The first module (upper left) performs current-to-voltage conversion and amplification; by selecting the appropriate resistor, the gain can be varied from a factor of 100 to a factor of 10^7. The second module (upper right) is a lowpass filter with a critical frequency of 1.6 Hz; any frequency above 1.6 Hz will be attenuated, thus eliminating noise with a higher frequency. The third module (lower) is a voltage reference and offset adjust. The voltage reference voltage is held constant by the Zener diode; The offset adjust variable resistor takes a portion of that voltage and feeds it to the lowpass filter as "ground"; the intent of this was to set the offset by changing the filter module's ground.

Upon construction and testing of this circuit, two problems were apparent. First, the gain settings were non-linear; the gain would increase by an inconsistent factor much larger than ten as

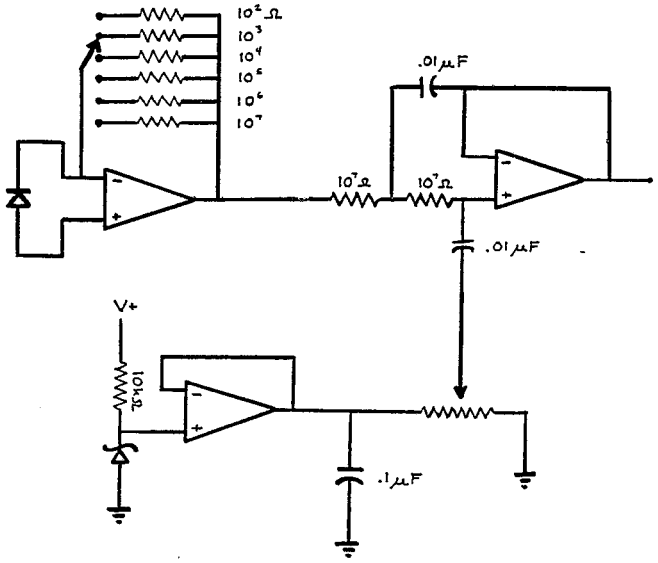

First Generation Electronics

Figure 2-11

the gain settings were traversed. Secondly, the offset adjust did not function. The first problem was discovered to be an error in the power supply to the integrated circuits. The circuit had been tested with ICs that required a power supply from positive voltage and ground, and built with ICs that required a power supply from positive and negative voltage. The second problem was that the ground for the filter module was not independent of ground for the rest of the circuit; when the offset was adjusted, the circuit rapidly compensated for the change, and no offset was seen.

Second Generation Circuit

The second generation circuit design is shown in Figure 2-12. The power supply modification is not shown. The offset adjustment is now effected by adding the offset adjust to the output of the first module in an additional op-amp stage; rather than use a manually altered variable resistor to change the offset, the offset voltage is supplied by the computer. The new op-am stage also functions as an amplifier with a gain of 100. The entire circuit has been constructed on a breadboard and mounted in a metal shielding case with standardized connectors for the photodiode input, power supply, and output to the computer.

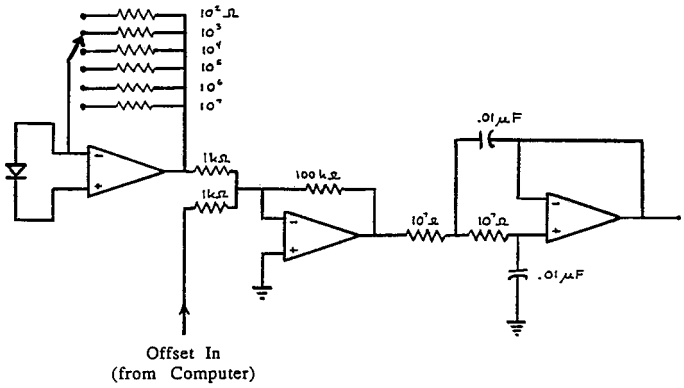

Second Generation Electronics

Figure 2-12

The Computer Interface

There are a number of advantages to using a computer for data acquisition, processing, and display. A computer can acquire and process the data much faster than a human being. The whole process can be automated. The two biggest advantages of using a computer interface, however, are the flexibility of data acquisition and processing and the easy jump to computer control of the instrument. Without a computer, data processing and display required dedicated electronics. If a user wanted to modify how the data was processed or displayed, it would be necessary to rewire physical circuits and/or build new ones. With a computer, only computer code must be modified. If the computer can generate electronic signals as well as read them, it becomes possible to control the instruments by the computer, and thus to automate even complicated experimental sequences.

The computer is a Macintosh IIci with a National Instruments NB-MIO-16XL data acquisition board and Labview II software. The Labview software is a graphical, icon-based programming language for data acquisition, processing, and display. The "language" is based on the concept of "virtual instruments", which function analogously to real instruments. Virtual instruments can also be combined to create higher-level virtual instruments. This hierarchical design conceals information about the internal workings of the hardware and software, while

making it easy to build new instruments specific to the application at hand.

The author has created a simple virtual instrument adapted to steady state acquisition. The block diagram - which shows the components of which the V.I. is built, most of which are actually built from more basic components - is shown in Figure 2-13. The front panel, which is the functional equivalent of the control panel of a physical instrument, is shown in Figure 2-14. This very simple V.I. has a sampling rate of approximately 100 Hz, and analyzes the collected signal for its maximum and minimum values, the mean, and standard deviation.

INSTRUMENT CHARACTERIZATION

In order to characterize our working instrument we use test substances. By making measurements on these test substances with both our instrument and a conventional instrument, we are able to compare the two instruments' capabilities. The test substance employed here is Methylene Blue.

Preliminary absorbance results obtained with the diode laser spectrometer are shown in Figure 2-15. This data was taken with the sample holder and first-generation electronics, with a Fluke 77 multimeter for readout. At the time this data was taken, the variable gain was not functioning correctly, as described in the

SSAcq with Offset
Wednesday, May 26, 1993 11:21 PM

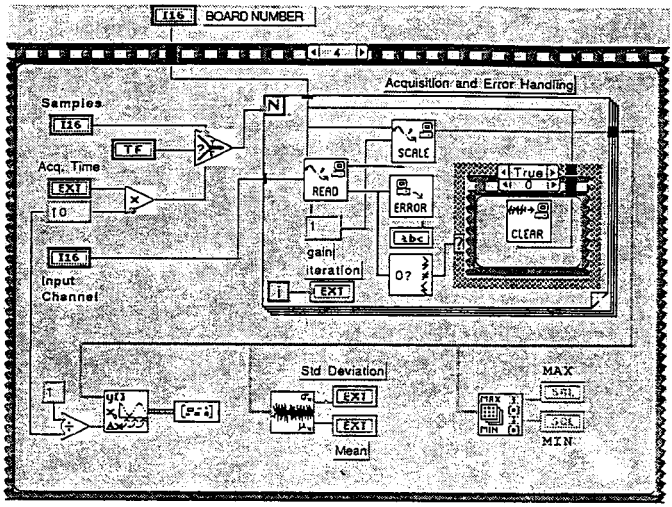

Virtual Instrument Block Diagram

Figure 2-13

Front Panel

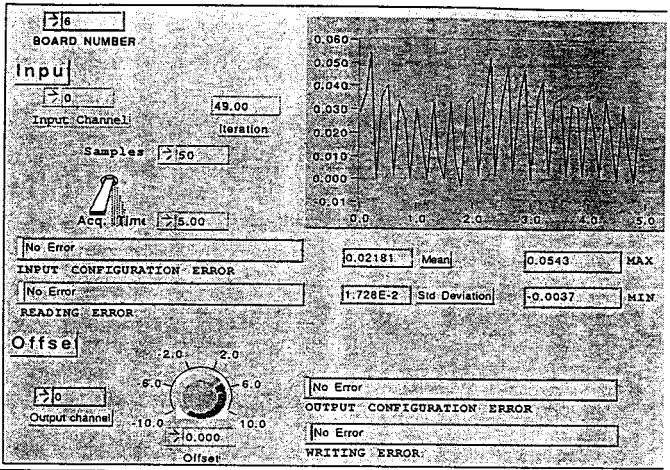

Block Diagram

Virtual Instrument Front Panel

Figure 2-14

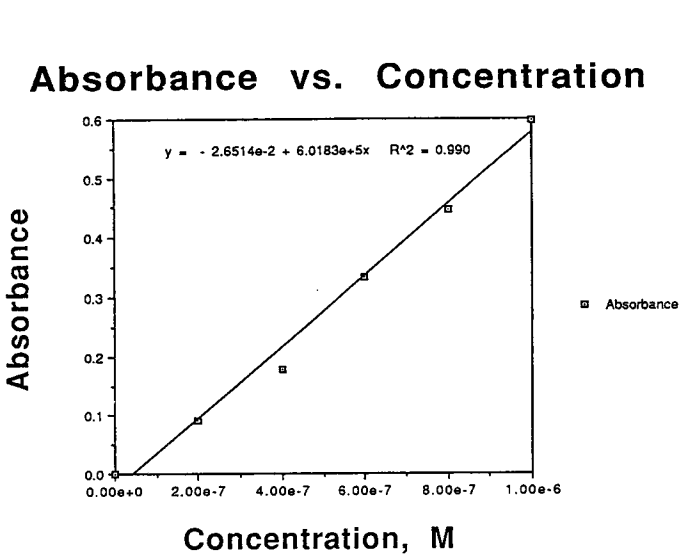

Preliminary Absorbance Results

Figure 2-15

Electronics section; therefore, the electronics limited us to only one order of magnitude in concentration. For comparison, the absorbances of the same solutions at several wavelengths were determined by a conventional UV/VIS spectrometer (Hewlett Packard 8452A Diode Array Spectrophotometer with a computer running HP 89531A MS-DOS UV/VIS Operating Software). The results are shown in Figure 2-16. The R^2 of the plots from the laser instrument and the diode array instrument are comparable; most of the deviation from perfect linearity stems from imprecision in the concentration of the solutions.

Preliminary fluorescence results are shown in Figure 2-17. Again, this data was taken with the sample holder, first-generation electronics, and Fluke 77 multimeter for readout. The filter used to block the laser wavelength was a #385 Royal Blue color filter (Edmund Scientific). At the time this data was collected, no optics of any kind were in place. The signal thus represents the portion of fluorescence (radiated in a random direction) that struck the detector surface. As the analysis in the Sample Holder section shows, the addition of a lens will increase the signal dramatically.

The variable gain problem has been fixed since this initial data was taken. A test of the response of the detector and electronics to light shows linear response over five orders of magnitude. (See Figure 2-18) We are limited at the bottom of the response range by the precision of the Fluke 77, which is +/- .001

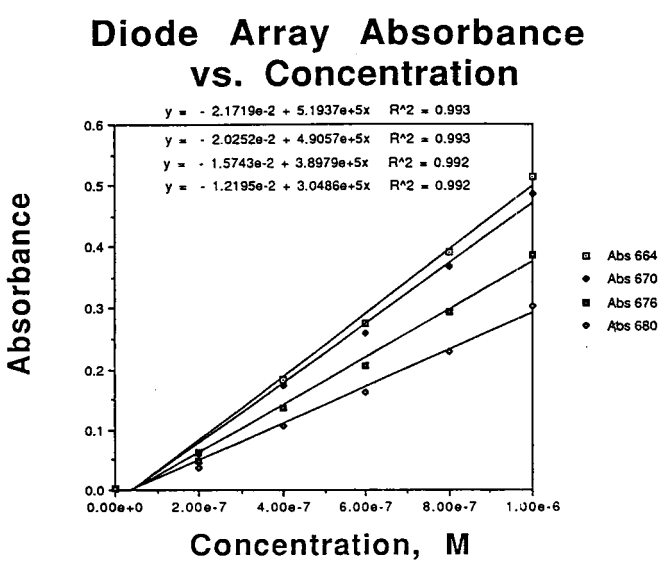

Diode Array Absorbance Results

Figure 2-16

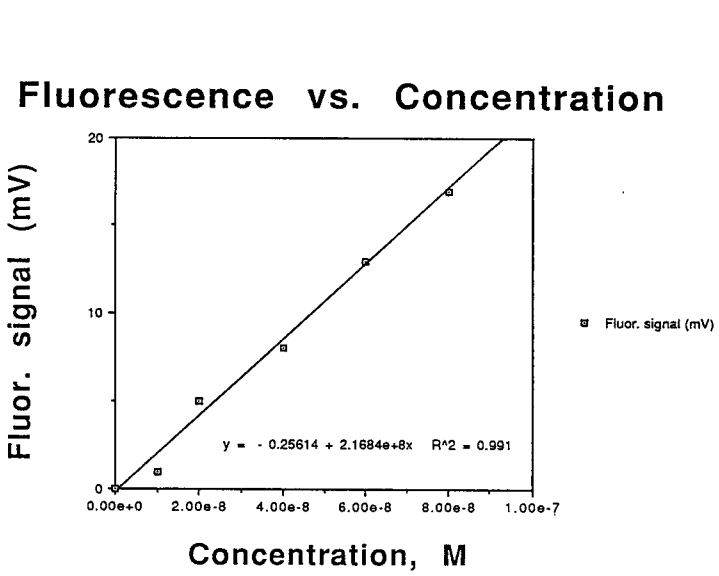

Preliminary Fluorescence Results

Figure 2-17

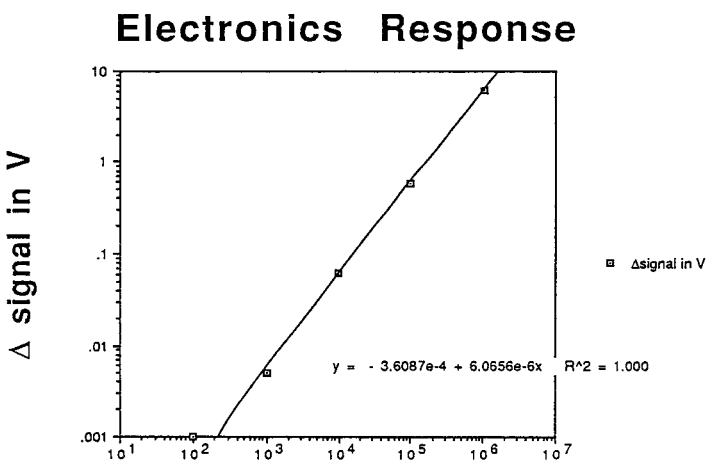

Linear Response of Electronics

Figure 2-18

V, and at the top of the response range by the capacity of our integrated circuits, which cannot output more than +/- 12 V.

As mentioned in Chapter 1, Methylene Blue is one of few compounds that absorb and fluoresce in the red end of the visible spectrum, and Sodium Dodecyl Sulfate is a good scatterer. The fact that the two molecules have other uses adds to the utility of our instrument. Because Methylene Blue is a good marker for RNA, DNA, and proteins, we should be able to stain and quantify biomolecules with our instrument.

FUTURE WO'

Work in progress includes the acquisition of absorbance and fluorescence data with the upgraded diode laser instrument. Because the gain now functions correctly, we now will be able to collect data over a much broader concentration range, and to test the instrument's detection limit. With optics installed and a new factor of 100 gain, we will have a much higher sensitivity. Comparison with conventional instruments will also be carried out. In order to collect scattering data, it will be necessary to widen two slots (in the input and scattering channels) by approximately 0.010 inch to accommodate line filters. Once this has been accomplished, scattering data will be obtained on our instrument and on a conventional instrument for comparison.

Another project in progress is the creation of dedicated Absorbance and Fluorescence/Scattering virtual instruments using the Labview software. These virtual instruments will be based on the Steady State Acquisition VI, which was constructed to be compatible with such an upgrade; both V.I.s will be capable of constructing a calibration curve and quantifying an unknown sample.

In the conceptual stage are plans for complete computer control over the electronics. This would involve a considerable increase in the complexity of the electronics. On the other hand, it would also allow practically simultaneous measurements of absorption, fluorescence, and scattering. Three photodiode detectors would be attached to the same circuit, and the computer would select which signal to monitor, which gain setting to employ, etc. The measurements of absorption, fluorescence, and scattering would not be truly simultaneous, but would follow each other at a very short (approximately 0.01 second) time interval. More primitively, three circuits could be built and interfaced to the computer.

A more difficult future project would be the creation of a new circuit, capable of time resolution. This would require the laser beam to be chopped or pulsed; because the current laser diode package includes a feedback stabilizer circuit, it cannot be electronically pulsed, but *could* be externally chopped (by q-switching, perhaps). For this application we would also need a

gated amplifier. Furthermore, our circuit would very likely have to be rebuilt using other methodology, because it is doubtful that we could find op-amps with a response time fast enough to handle time resolution on the nanosecond time scale. (13 V/μs is considered a *high* slew rate;[6] any faster-changing signal would be distorted.)

LITERATURE CITED

1. Atkins, P. *Physical Chemistry;* Freeman: New York, 1990; p 694.

2. Skoog, D. *Principles of Instrumental Analysis, 3rd Ed;* CBS College Publishing: New York, 1985; p 235

3. Lerner, J.; Thevenon, A. *The Optics of Spectroscopy;* Instruments S.A., Inc: Edison, 1988; p 14-15

4. Mims F. *Engineer's Notebook II;* Radio Shack: U.S.A., 1982.

5. Mims F., *Engineer's Mini-Notebook;* Radio Shack: U.S.A., 1985.

6. *Semiconductor Reference Guide;* Radio Shack: Forth Worth, 1988.

CHAPTER III:

CHARACTERIZATION OF THE METHYLENE BLUE/ SODIUM DODECYL SULFATE CHEMICAL SYSTEM.

MOTIVATION

As mentioned in Chapter 2, Methylene Blue and Sodium Dodecyl Sulfate are useful test reagents for characterization of the diode laser spectrometer. However, they also comprise a chemical system that is interesting in its own right. The findings of a study of this chemical system are presented in this chapter.

Methylene Blue is a dye, and Sodium Dodecyl Sulfate is a surfactant. Methylene Blue is commercially available as a positively charged molecule with Chloride as a counter-ion. (See Figure 3-1) Methylene Blue is highly water soluble for a dye; it is soluble up to 4% in water.[1] Sodium Dodecyl Sulfate (See Figure 3-2) is a micelle-forming anionic surfactant. Below a certain concentration, micelle-forming surfactants exist primarily as monomers. However, when the concentration reaches a sharply defined value called the *critical micelle concentration* (CMC), the molecules aggregate to form micelles.[2] (See Figure 3-3)

Both of these general categories of molecules are members of a still more general category: both dyes and surfactants are *amphiphiles*. Amphiphiles are molecules that possess both hydrophilic and hydrophobic moieties. Amphiphiles are common in nature, and especially so in biochemistry: proteins, DNA/RNA, and membrane-forming lipids are all amphiphiles. In all of these

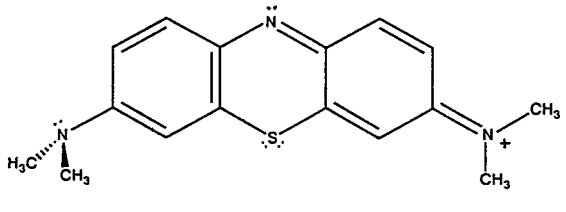

Methylene Blue

Figure 3-1

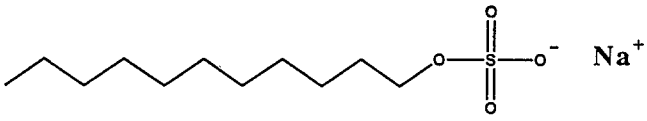

Sodium Dodecyl Sulfate

Figure 3-2

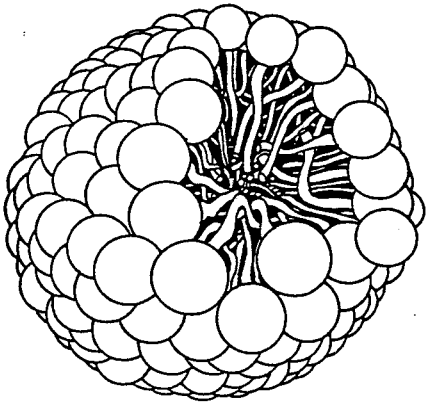

Fig. 23.17 A representation of a spherical micelle. The hydrophilic groups are represented by spheres, and the hydrophobic hydrocarbon chains are represented by the stalks: the latter are mobile.

Adapted from Atkins, *Physical Chemistry*, p 708

Micelle

Figure 3-3

examples, the amphiphilic character of the molecules has a profound impact on their behavior. Because there are *both* hydrophilic and hydrophobic moieties in the molecule, the solute-solvent system cannot minimize its energy simply by partitioning itself into aqueous and non-aqueous phases as in the case of, say, hydrocarbons in water. Instead, the molecules seek the global energy minimum (of the solute and solvent) by changing their conformation - folding, as in the case of proteins, DNA, and RNA - or by associating themselves with their neighbors - as in the case of membrane-forming lipids and micelle-forming surfactants.

It is no overstatement, then, to say that the interplay of interactions that drives the conformation changes and associations (inter- and intra- molecular) is important and vital. Unfortunately, this interplay of interactions is not very well understood. Protein folding and DNA conformation, for instance, are both classic problems.

This is the ultimate reason that we study dye-surfactant interactions. Surfactants are really the simplest amphiphiles, with only one hydrophilic and one hydrophobic region. It is well known that the environment of a dye molecule influences its spectra.[3] In particular, interaction with a surfactant will induce spectral changes. Dye molecules therefore offer us the opportunity to probe the interaction of amphiphilic molecules optically. If we can understand the interactions between dyes and surfactants and the mechanism(s) of the induced spectral

changes, we could begin to use dye molecules as a probe of the amphiphile - amphiphile interactions in more complicated situations, such as proteins or membranes. This is the long term goal.

Dye-surfactant interactions are of immediate practical import in analytical chemistry, where dyes are used as detectible tags in systems that make use of surfactants.[4] An example might be gel electrophoresis (which uses SDS to give proteins a negative "charge coat"), where the results are visualized by staining with Methylene Blue (which is a common biomarker). Finally, dye-surfactant interactions are an unsolved and challenging puzzle, and good exercise for simple curiosity.

Methylene Blue and Sodium Dodecyl Sulfate are good choices for a study of dye-surfactant interactions. SDS is a commonly used surfactant and is well characterized.[5,6] Micelle-formation is normally an aqueous phenomena, and most biologically interesting amphiphiles are in aqueous solution, so we also need a water-soluble dye. Methylene Blue is one of only a few dyes that are significantly soluble in water, so it is a good choice in this regard (in addition to absorbing at the diode laser's wavelength.)

STRATEGY

In order to elucidate the nature of the interaction between SDS and Methylene Blue, a "2 + 2 = 5" strategy was employed. For any given spectral characterization technique, we need to take a spectrum of Methylene Blue alone, a spectrum of SDS alone, and a spectrum of Methylene Blue and SDS together. Any features in the spectrum of the mixture that were not present in the spectra of either of the two alone (or the abscence of any features present in the spectra of either of the two compounds alone in the spectrum of the mixture) must be due to an interaction between the two.

EXECUTION

In accordance with the strategy presented above, Methylene Blue, Sodium Dodecyl Sulfate, and mixtures of the two have been characterized by UV/VIS absorbance, fluorescence, and HNMR. Characterization was also attempted by HPLC and ^{13}C-NMR. UV/VIS absorbance measurements were taken on a Hewlett Packard 8452A Diode Array Spectrophotometer with a computer running HP 89531A MS-DOS UV/VIS Operating Software. Fluorescence data was collected with a Perkin Elmer LS-5B Luminescence Spectrometer. Fluorescence lifetimes were measured with a Photon Technology International LS-100 Luminescence System. NMR spectra were taken with a Gemini

200 NMR system. The HPLC characterization attempt was terminated when it was discovered that SDS stuck to the column prefilter. The ^{13}C-NMR characterization failed due to lack of signal; the maximum concentrations of MB and SDS in water were too low to give sufficient signal.

In this section, the salient features of the structure and spectra of Methylene Blue alone and Sodium Dodecyl Sulfate alone will be analyzed and synopsized, followed by the analysis of SDS and Methylene Blue together.

Methylene Blue

Structure and Properties

The structure of Methylene Blue, including the hybridization of the atomic orbitals, is shown in Figure 3-4. Like most dyes, Methylene Blue has a highly conjugated ring system. If we think in terms of a "particle in a box" model, the π bonding network forms a large "box" for the electrons; this lowers the energy levels and decreases the energy necessary to make a transition.[7] Thus, the absorption of the molecule shifts toward the red. Because the π-system is large, a small variation in electron density also produces a large change in dipole moment. Thus the dipole moment change of a conjugated ring system tends to be large, and the molar absorptivity is correspondingly very high.[8] Methylene Blue, in addition to being highly conjugated, is also a rigid

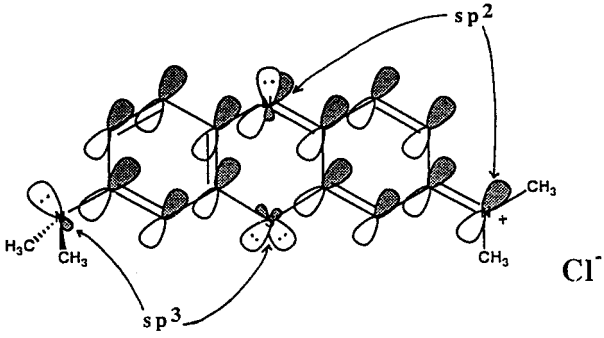

Methylene Blue

Figure 3-4

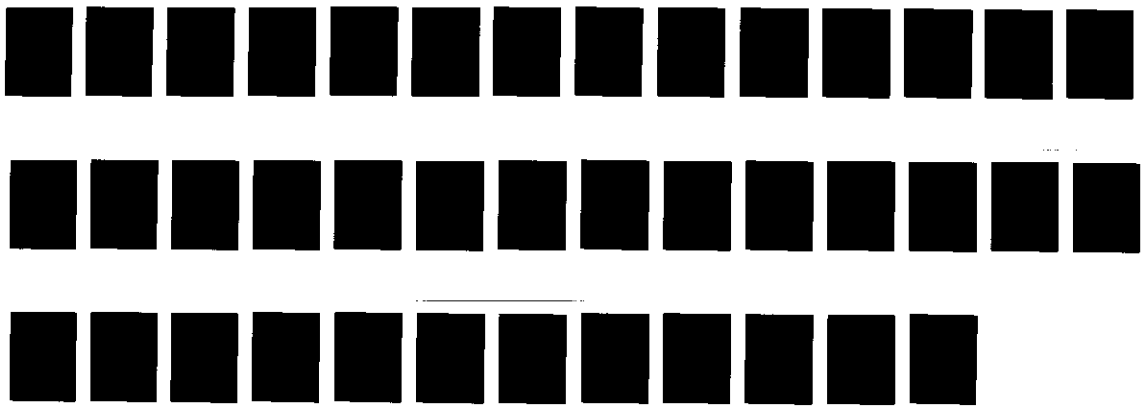

molecule; this rigidity plays a role in increasing the quantum yield for fluorescence.[9]

The absorbance and fluorescence spectra of Methylene Blue at a concentration of 10^{-6} M in water are shown in Figure 3-5 and 3-6, respectively. The salient features of the absorbance spectrum are the peak at 664 nm (and its shoulder labelled at 610 nm), and the peak at 292 nm; The peak at 246 nm stayed constant under all conditions. By analogy with the band structure of benzene, the peak centered at 664 nm will be called the B band, and that at 292 nm the E_2 band. The main feature of the fluorescence spectrum is the large peak at 688 nm, which will be referred to as the F band. The 492 nm peak is simply second order scattering from the diffraction grating in the monochromator.

HNMR and 2D-HNMR spectra of Methylene Blue 1% (approx 3.1×10^{-2} M) in D_2O are shown in Figures 3-7 and 3-8, respectively. The d = 4.7 peak is due to H_2O; By the peak integrations, the d = 3.0 peak must be the methyl protons. The lone H must correspond to the remaining singlet at d = 6.55, and the remaining two are assigned by reference to the literature.[10] Obviously, the concentration is much higher than that used for the visible spectral samples.

Methylene Blue 10^{-6} M

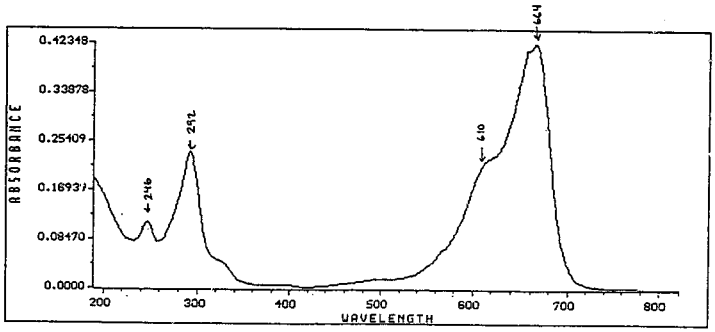

Methylene Blue Absorption Spectrum

Figure 3-5

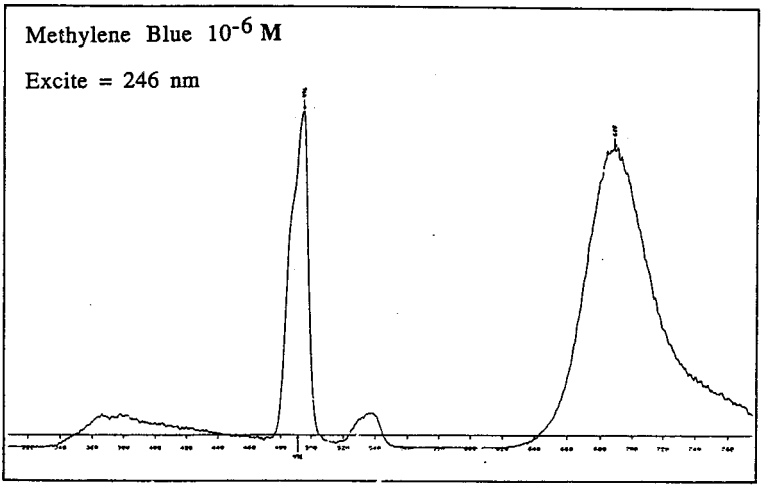

Methylene Blue Fluorescence Spectrum

Figure 3-6

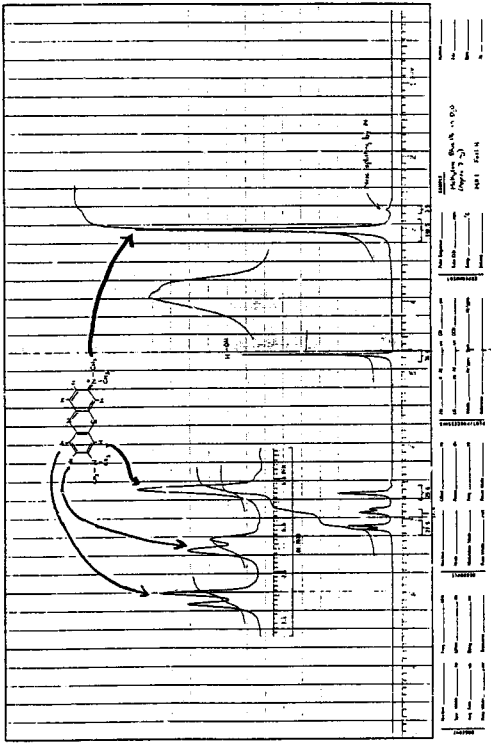

Methylene Blue NMR Spectrum

Figure 3-7

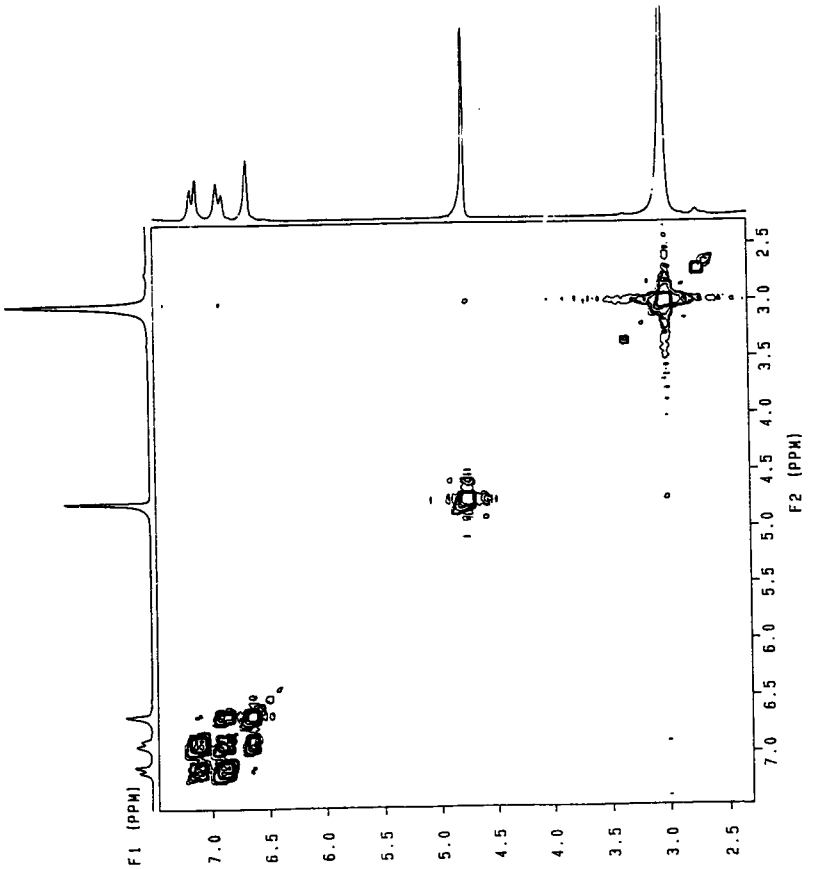

Methylene Blue 2D-HNMR Spectrum

Figure 3-8

Energy Level Structure

In order to get as much information as possible from the spectral changes, we need to have an idea as to what structural features are responsible for what features of the energy level diagram. By applying the known property that the molar absorptivities for n -> π^* transitions are usually low and those for π ->π^* are usually high,[11] we can determine that the absorption bands that we are looking at, being very intense, are π ->π^* transitions. We must concern ourselves mainly with the π system of the molecule. Using the LCAO-MO approximation, we can start with the (atomic) p orbitals perpendicular to the plane of the ring and construct 12 (molecular) π-system orbitals, just as can be done with benzene. (See Figure 3-9.) Because Methylene Blue is a much more complex molecule than benzene, it would actually take a computer program to generate the molecular orbitals. However, the energy level diagram will be *qualitatively* similar, and it is this qualitative similiarity that we will make use of; see Figure 3-10. Keep in mind that the higher the energy level, the more nodes it will have.

In general, π ->π^* transitions undergo red shifts with increasing solvent polarity. The effect is due to dipole/induced-dipole forces, which lower the energy levels of both HOMO and LUMO states. However, the higher energy state's energy is usually lowered more, so the transition energy decreases and the absorption shifts towards the red.[12] Because water is a very

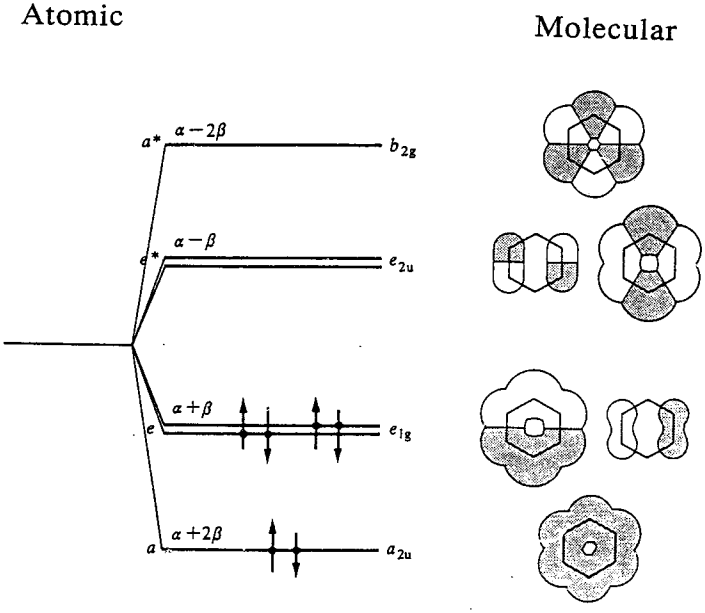

Adapted from Atkins, *Physical Chemistry*, p 418

Atomic to Molecular Orbitals

Figure 3-9

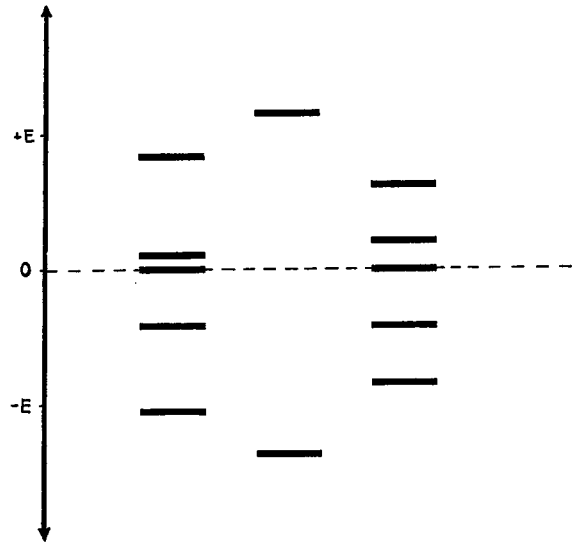

Qualitative Energy Level Diagram
For Methylene Blue

Figure 3-10

polar solvent, we expect that the spectrum of MB in water will already have redshifted; in less polar solvents, the redshift will be smaller. Thus, we should see a blue shift in less polar solvents. As will be described below, this effect is most clear in the B band.

The E_2 band is also influenced by the *auxochrome effect*; an auxochrome is a substituent (on a conjugated ring system) that has a nonbonding electron pair. Donation of the electrons to the ring apparently stabilizes the π^* state, producing a red shift.[13] From this, we expect that if the nonbonding pair is complexed (as it should be in water), the absorption should shift to the blue; we should see a red shift in less polar solvents. In the case of Methylene Blue, the $-N(CH_3)_2$ group is the auxochrome. The B band is clearly dominated by the solvent polarity effect. Apparently, the solvent polarity effect and the auxochrome effect fight for dominance in the E_2 band. This is illustrative: we would expect to see that more highly excited states have more nodes, and this implies that electron density is confined to a smaller region. This in turn suggests that local effects (substituents, for instance) should influence this localized electron density more than the rest of the molecule. The E_2 band represents a transition to a higher energy level and therefore displays a more localized effect.

Concentration and Solvent Polarity Effects

The dependence of the visible spectra on concentration and solvent polarity was investigated. Figure 3-11 shows absorption spectra taken in H_2O, MeOH, and EtOH at two different concentrations; the low concentrations are grouped together on one page, the higher concentrations on the other. Several pieces of information can be extracted from these spectra. Examining the changes in the the spectra vs. increasing concentration, we see that the dominant effect is for the "shoulder" corresponding to 610 nm in H_2O (the B_2 band) to grow at the expense of the B band. Because there are only solvent and Methylene Blue in the solutions, all the peaks must be due to Methylene Blue. However, the B and B_2 bands must be due to different species, because otherwise they would retain their relative intensity to one another. (It is difficult to imagine a global change in concentration causing one radiative decay mode to be preferred over another. It is much more likely that the spectral change is due to a change in local environment.) The logical conclusion is that the B band is from a free dye molecule in solution, while the B_2 band is from dye dimers. Braswell, using data-fitting techniques applied to spectroscopic data, found that Methylene Blue associates further at higher concentrations, forming a B_{inf} band that assymptotically approaches 590 nm.[14]

Examining the effect of solvent polarity, we see that as solvent polarity decreases, there is less tendency towards growth

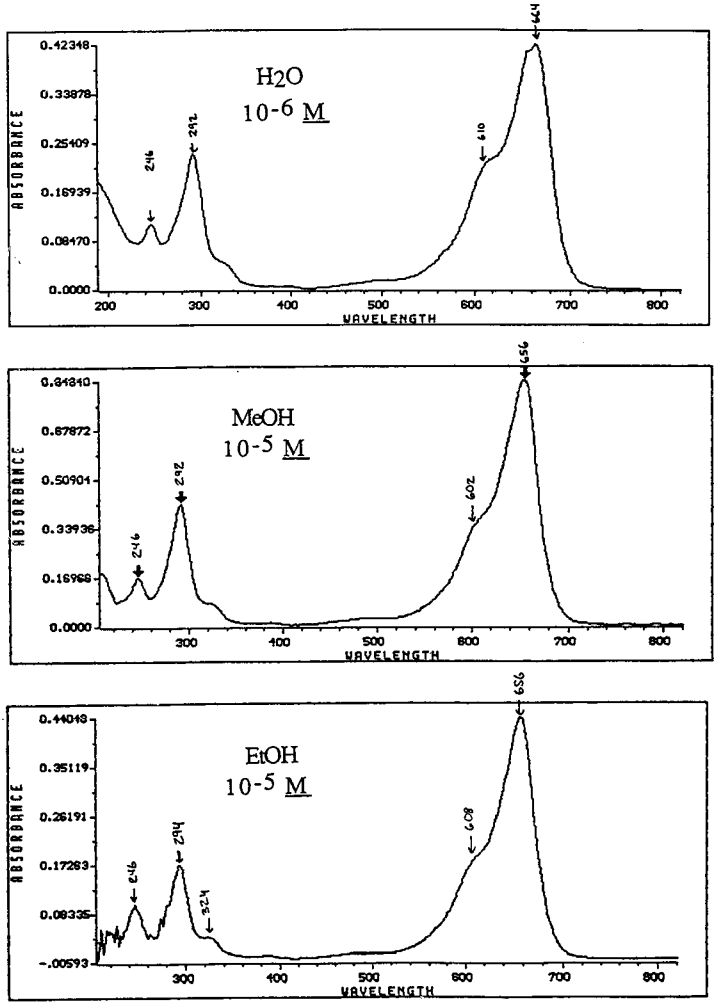

Methylene Blue Absorption Spectra

Figure 3-11

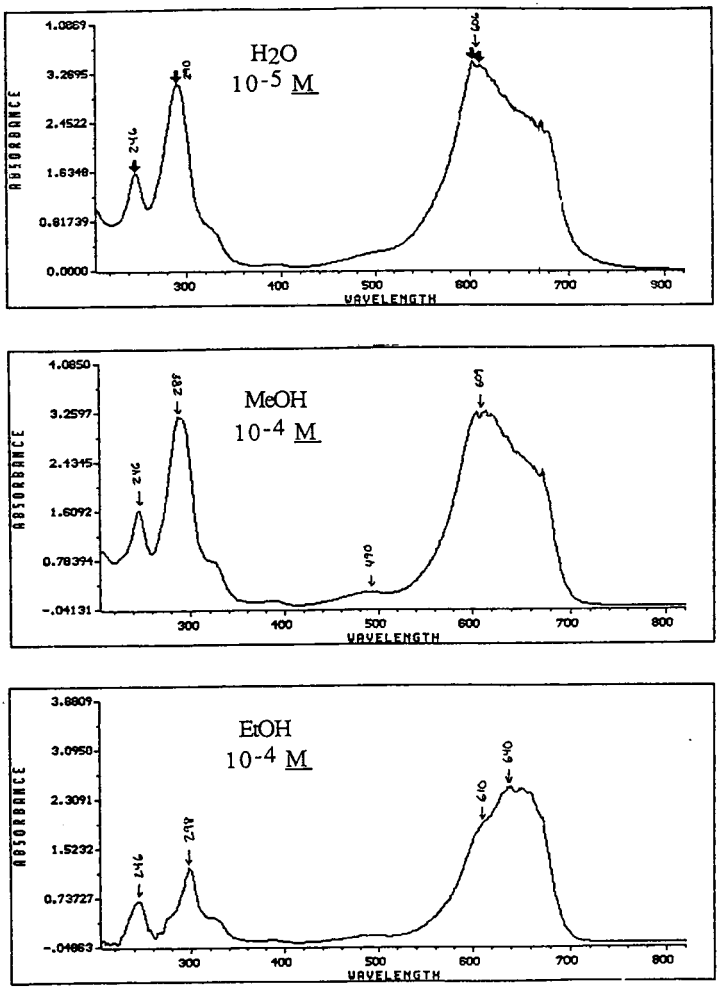

Methylene Blue Absorption Spectra

Figure 3-11

of the B_2 band at the expense of the B band. This is most easily explained if we assume that the formation of the dimers is hydrophobically driven. (See below)

A word about the hydrophobic effect is in order here. The mechanism of the hydophobic effect is energy minimization of the *solvent*; in order to form as many hydrogen bonds as possible, the area of contact with non-hydrogen-bond-forming (hydrophobic) moieties must be minimized. This is accomplished by pushing the hydrophobic moieties together. The network of hydrogen bonds around the hydrophobic "island" thus formed keeps the hydrophobic moieties together, and can be loosely considered a hydrophobic "force".[15] In the specific example considered here, we can see that as the solvent polarity decreases, there will be less tendency for the solvent to form hydrogen bonds, and therefore less tendency for the hydrophobic moieties to be pushed together. Fewer dimers would be formed, in accordance with the observed results.

Mechanism of Spectral Changes

From the shift in the absorption spectrum we see that the energy difference between the ground and excited states of the dye dimer is larger than for the monomeric form. On the other hand, the *fluorescence* of the dimer is exactly the same as that of the monomer. This can be explained by postulating that the excited state is also vibrationally excited, and pushes away its

companion dye molecule before fluorescing. The time scales involved (10^{-15} s for a molecular vibration, 10^{-9} s for fluorescence) indicate that there is time for this to occur.

Given that dimers do form, how does dimer formation influence the spectrum of the dye? Clearly, there must be either more stabilization of the ground state than of the excited state, or more destabilization of the excited state than of the ground state. The best explanation for the energy gap increase is that the Methylene Blue molecules associate by stacking, as in Figure 3-12. Observe the overlap of the π-systems. If both molecules are in their ground state, the overlap of the M.O.s will be positive everywhere, as in 3-12a. This represents a stabilization of the ground state for both molecules. On the other hand, if one electron is excited to an antibonding M.O., it will have net zero overlap with all the bonding M.O.s, as in 3-12b. Although the Figure shows only one M.O. per molecule, in reality all 6 bonding M.O.s would be involved; for simplicity, the unchanged M.O.s are not shown. Also, the M.O. shown is not really the HOMO; it is used for illustrative purposes. The point is that the excited M.O. will have more nodes than the unexcited M.O., and therefore not stabilize it.

This model also generalizes to many other dyes, since a planar, conjugate π-system is common. In addition to being theoretically pleasing, this model is also supported by direct observation: the solid dye has a metallic sheen, indicating that it

a. 2 Ground States

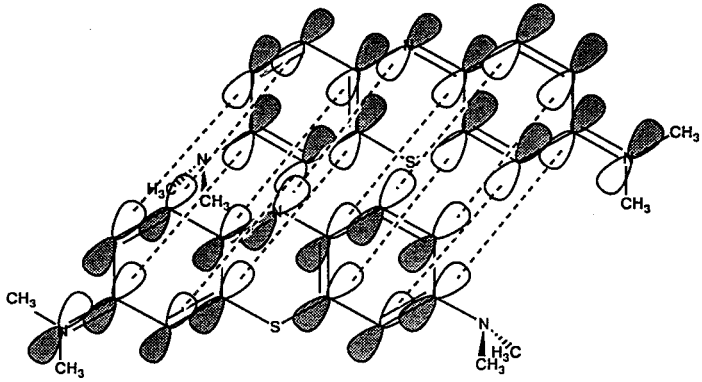

b. 1 Ground, 1 excited

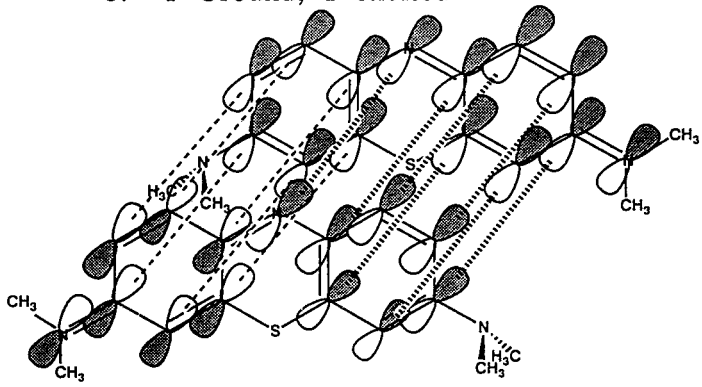

Stacked Methylene Blue Molecules

Figure 3-12

is probably a conductor, as we would expect from an extended conjugate π-bond system! Two other dyes on hand in our lab, Nile Blue Perchlorate and Methyl Violet (See Figures 3-13 and 3-14), *also* have a metallic sheen in solid form, although they have very different structures than Methylene Blue. Other dyes seem to follow the pattern.

Sodium Dodecyl Sulfate

Structure and Properties

The structure of Sodium Dodecyl Sulfate is shown in Figure 3-2. (Sodium Dodecyl Sulfate is also known as Sodium Lauryl Sulfate, and is variously abbreviated as NaDDS, NaDS, NaLS, and (here) as SDS.) As it has no conjugated double bonds, we expect that it will not absorb in the visible spectrum. However, it forms aggregates, so it is a good light scatterer, and this has an effect on the absorption spectrum; light that is scattered does not reach the detector, and is interpreted as an absorbance. This "mock absorbance" is displayed in Figure 3-15.

The H-NMR spectrum of SDS (10^{-2} M) in D_2O is displayed in Figure 3-16. The triplet at d = 1.2 ppm represents the methylene groups in the hydrocarbon tail. The d = 4.75 ppm peak is H_2O. The peak at d = 4.0 is presumed to be due to the methylene group closest to the polar sulfate head. With a $-CH_2-$ group surrounded by $-CH_2-$ groups, we *expect* a 1:4:6:4:1 quintet; either the

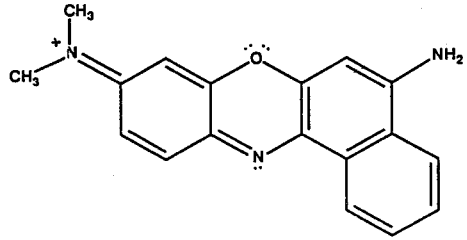

Nile Blue

Figure 3-13

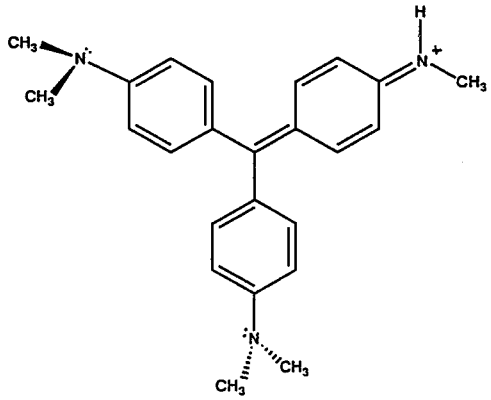

Methyl Violet

Figure 3-14

Sodium Dodecyl Sulfate 10^{-3} M

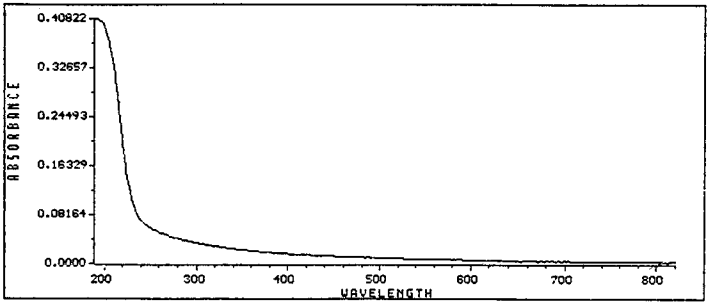

Mock Absorbance of SDS

Figure 3-15

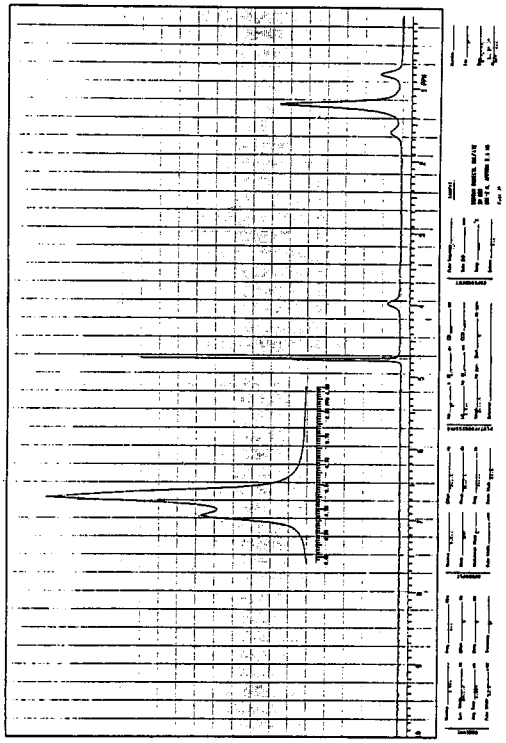

SDS NMR Spectrum

Figure 3-16

molecule is long enough for the methylene group to consider its nearest neighbor methylene groups chemically equivalent, or the broadening effect has reduced the intensity of the satellite peaks and rendered the outlying peaks invisible. The concentration is well above the CMC, in order to provide a sufficient concentration of hydrogen nuclei. The broadening of the peaks may be attributed to the distribution of environments that any given hydrogen experiences; in the NMR of a powdered solid, the dipole moments affecting the molecules do not average to zero as they do in solution. This results in extensive peak broadening.[16] A similar rationale may be used to explain the broadness of the micellar SDS resonances.

The critical micelle concentration for SDS is 0.234% in water (8.11×10^{-3} M).[17] If we assume that the micelles are formed by stepwise aggregation,

$$\begin{aligned} SDS + SDS &\Longrightarrow (SDS)_2 && K_1 \\ (SDS)_2 + SDS &\Longrightarrow (SDS)_3 && K_2 \\ (SDS)_3 + SDS &\Longrightarrow (SDS)_4 && K_3 \\ & \cdots \\ (SDS)_{n-1} + SDS &\Longrightarrow (SDS)_n && K_n, \end{aligned}$$

then by adding all of these steps we get

$$n\,SDS \Longrightarrow (SDS)_n \qquad K = \Pi K_i.$$

We can see that $[(SDS)_n] = K[SDS]^n$. For an SDS aggregation number n of approximately 64,[18] the formation of full micelles is thus dependent on the 64^{th} power of the SDS concentration! This is why the critical micelle concentration is so sharp.

Methylene Blue in Sodium Dodecyl Sulfate

There are four basic questions which we can ask about the interactions of Methylene Blue and Sodium Dodecyl Sulfate:

1) What occurs?
2) Why does it occur?
3) What spectral changes are there?
4) What is the mechanism for the spectral changes?

This section will first present the basic observations, then attempt to answer these questions for the MB-SDS system a) below and b) above the critical micelle concentration. Instead of presenting the morass of competing models for what occurs, the model that best explains the facts is presented, and the evidence supporting it explained.

At this point in our investigation, we are examining the "5" in our "2 + 2 = 5" strategy. As the vast majority of solutions examined have [MB] = 1.0×10^{-6}, we expect that our dye molecules will be primarily in their monomer form, with only a small proportion of dimers.

Observations

The dependence of the Methylene Blue absorption spectrum on SDS concentration is illustrated in Figure 3-17. The spectrum remains constant for [SDS] <= 10^{-4}. Above this concentration, there is a progressive blue shift in the absorption until the concentration reaches 5 x 10^{-3} M. At this concentration and higher, the absorption spectrum appears almost identical to that of the uncomplexed dye monomer. Visually, Methylene Blue at a 10^{-6} M concentration is sky blue; as the concentration of SDS increases, it turns light blue/purple, then violet, and then back to sky blue. This visual shift is the basis for the Spectral Change Method for determining the CMC;[19] the assumption that is made in this method (which is, as will be shown presently, erroneous for a number of reasons) is that the color change indicates micelle formation.

The fluorescence spectrum undergoes a similar pattern of changes, although the specific effects are different; see Figure 3-18. The spectrum changes little at low SDS concentrations, undergoes a dramatic change, and then returns almost completely to its pre-SDS appearance.

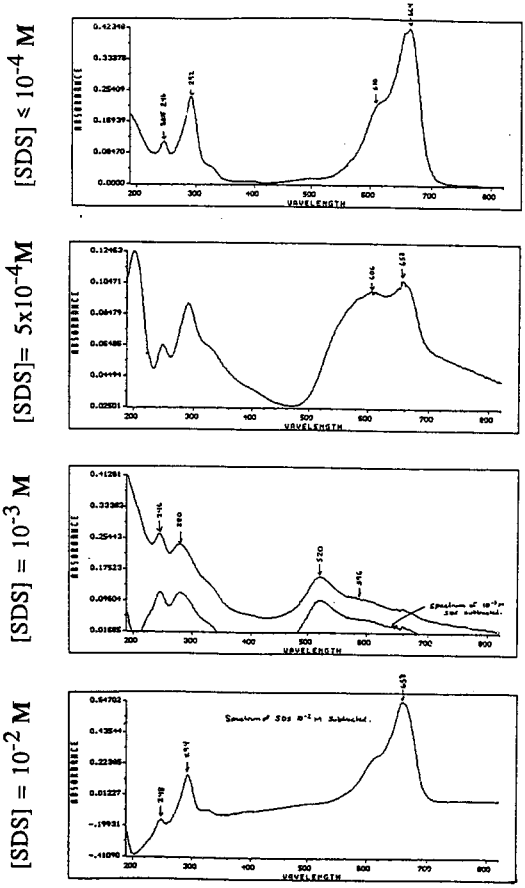

Methylene Blue Absorption Spectra as a Function of SDS Concentration

Figure 3-17

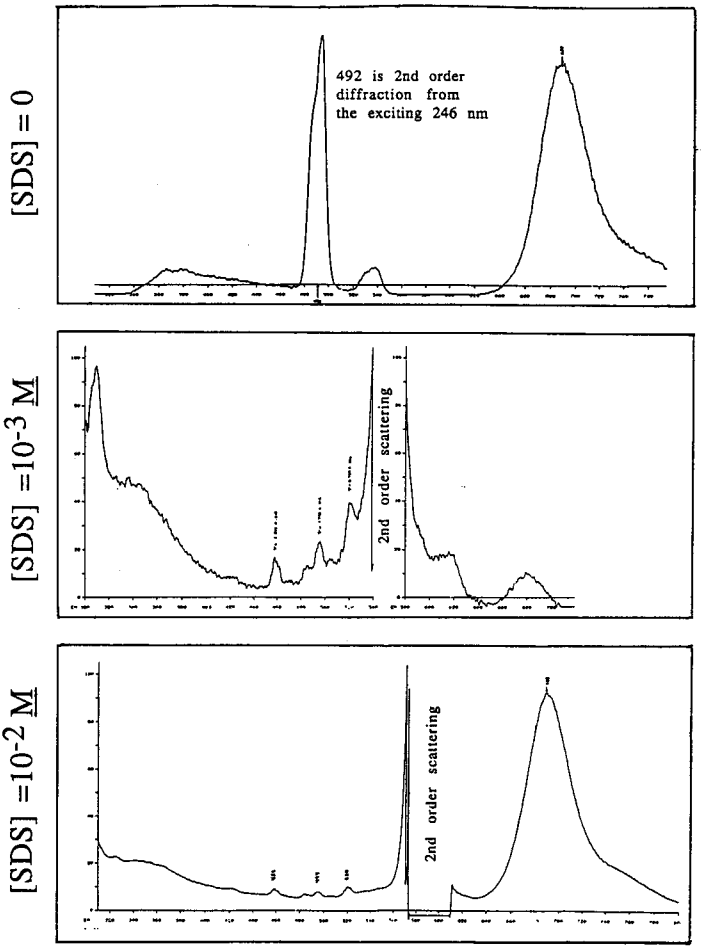

Methylene Blue Fluorescence Spectra as a Function of SDS Concentration

Figure 3-18

Below the CMC

Primary Effects

Below the CMC, two effects are important: formation of a water-insoluble stoichiometric complex between Methylene Blue and SDS (DS^- is the Dodecyl Sulfate anion)

$$MB^+ + DS^- \Longrightarrow [MB\text{-}DS],$$

and solubilization of this insoluble complex by SDS molecules:

$$[MB\text{-}DS] + SDS^- \Longrightarrow [MB\text{-}DS]DS^- + Na^+$$
$$[MB\text{-}DS]DS^- + SDS^- \Longrightarrow [MB\text{-}DS]DS^-_2 + Na^+$$
$$[MB\text{-}DS]DS^-_2 + SDS^- \Longrightarrow [MB\text{-}DS]DS^-_3 + Na^+.$$

The evidence for formation of an insoluble complex is direct. We observed the effect serendipitously in our lab, and found it confirmed and more intensively analyzed by Murkerjee and Mysels.[20] They found that for solutions where [MB] >= [SDS], a fine precipitate formed; Elemental analysis of this precipitate showed conclusively that its stoichiometric ratio was 1:1.

Mukerjee and Mysels then conclude that the absorption blue-shift is due to the formation of this insoluble dye-surfactant salt, and that the redshift on further increase of SDS concentration is due to the solubilization of the salt by SDS. This is both illogical

and incorrect. If the electrostatic interaction is the cause of the spectral blueshift, then it is illogical to expect simple solubilization by SDS, which will not alter the electrostatic effect significantly, to explain the subsequent redshift. Furthermore, the electrostatic explanation is incorrect, because it is now known[21] that the association of a charged dye with counterions (even very bulky counterions) does not change the spectrum of the dye.

Since solutions of MB and SDS with SDS in excess do not form a precipitate, the MB-DS salt must be better solubilized in them. We also have spectral evidence for the association of SDS molecules with our salt. From the absorption spectra (See Figure 3-17), we see that there is a blue shift in both the E_2 and B bands, and a loss of intensity of the B band. It is also apparent that the shift moves *progressively* downfield with increasing SDS concentration, in a manner analagous to the blueshift occuring from progressive oligomerization of MB; this indicates that the blue shift may also be due to a progressive association. The more SDS molecules associated with a MB-DS complex, the larger the blue shift.

The fluorescence spectrum of MB in SDS 10^{-3} M provides an even stronger clue. There are two effects present. First, the fluorescence F band undergoes an 8 nm blueshift and a near complete loss of intensity. Second, three sharp peaks appear, at 460, 496, and 520 nm. The wavelengths of these three peaks do not depend on the excitation wavelength. From this information

alone, we cannot determine whether these peaks are three new fluorescence peaks from *one* species, or the superposition of peaks from *three different species*.

Measurement of the fluorescence lifetime of these three peaks yields strong evidence that the peaks are due to separate species. The lifetimes are measured to be

460 nm: 2.244 (+/- .013) ns
496 nm: 1.420 (+/- .012) ns
520 nm: 0.789 (+/- .006) ns

We expect the fluorescence lifetimes of different peaks in the same compound to be nearly identical. If anything, we would expect to see a slight increase in the fluorescence lifetime as wavelength shortens, because the molecule must relax (via internal conversion) further before making a radiative transition. Because internal conversion is so fast (on the order of 10^{-12} seconds) compared to fluorescence (10^{-9} seconds), this influence should be neglible. Because the lifetimes of the fluorescence peaks *decrease* with increasing wavelength, we conclude that the peaks must be due to different species. If we make the reasonable assumption that association of an SDS molecule with the MB-DS complex would reduce the amount of jostling from the solvent, thus increasing its fluorescence lifetime, then the 460, 496, and 520 nm peaks would correspond to the most, less, and least SDS-associated species. Because the peaks are discrete

rather than being continuous, we assume simply that the 460, 496, and 520 nm peaks are due to MB-DS with three, two, and one associated SDS molecules, respectively.

Mechanism of Effects and Spectral Changes below the CMC

The mechanism of formation of the MB-DS complex is the formation of an ionic bond. This fits chemical intuition. Methylene Blue is singly positively charged, while the Dodecyl Sulfate anion is singly negatively charged. Apparently, formation of an ionic bond between a charged chromophore and an oppositely charged ion has no effect on the relative spacings of the chromophore's energy levels. This can be rationalized by noting that in a pure ionic bond, electron density is not altered; the stabilization comes from simple coulombic attraction, and the entire chromophore is presumably in a state of lower potential energy. See Figure 3-19.

The mechanism of the aggregation of SDS with the MB-DS complex is the hydrophobic effect. Because MB-DS has no exposed charges with which water can complex, it is clearly more hydrophobic than MB^+ or DS^-. SDS is a surfactant, and we already know that surfactants aggregate with hydrophobic molecules by the hydrophobic effect, for reasons discussed earlier (See the "Concentration and Solvent Polarity Effects" topic in the Methylene Blue section.) Once the two molecules are brought together by the

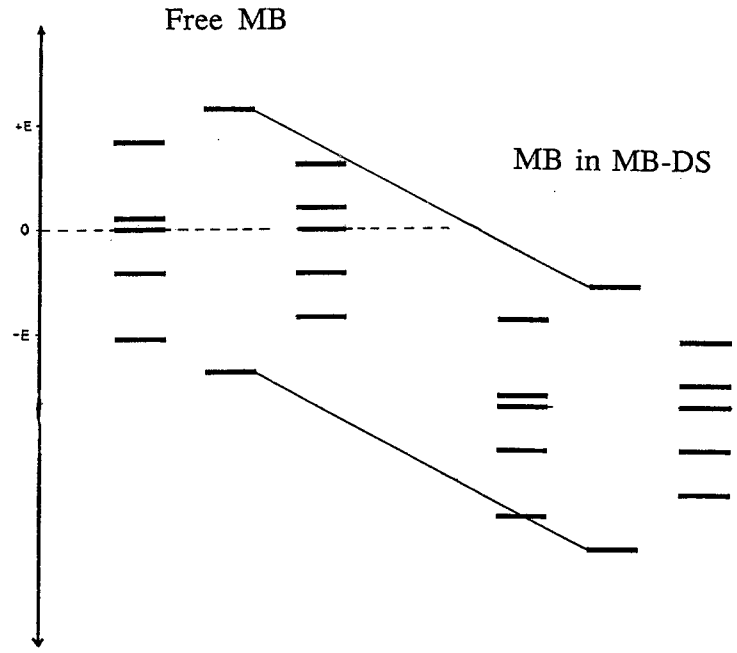

Energy Level Shifts for
$MB^+ + DS^-$ ==> MB-DS

Figure 3-19

hydrophobic effect, they can also be attracted to each other by dipole-dipole, dipole-induced dipole, or Van der Waals forces.

The mechanism of the spectral change induced by the hydrophobic association is more difficult to deduce. The author's tentative hypothesis is based on the polarizability of the π-electron cloud on Methylene Blue. Simply put, the more nodes a molecular orbital has, the more tightly localized the electron density is, and the more difficult it will be to polarize that electron density by dipole-induced dipole or Van der Waals forces. (See Figure 3-12.) The formation of a Van der Waals (VDW) bond represents a stabilization of the ground state and the excited state, but the ground state will be stabilized more. Assuming that the magnitude of the stabilization is at least as large as the change in the energy required to induce the transition,

$$\begin{aligned} \Delta H_{stab} &\geq h\nu_{B,after} - h\nu_{B,before} \\ &\geq hc/\lambda_{B,after} - hc/\lambda_{B,before} \\ &\geq hc/520nm - hc/664nm \\ &\geq 47.7\ kJ/mol\ . \end{aligned}$$

This does appear to be large for Van der Waals bonding. However, Methylene Blue is a large, planar molecule, and SDS has a long, simple hydrocarbon chain; The two could pack (and form VDW bonds) very efficiently. With 3 SDS molecules, the effect could be very large. (Velcro is another good example of a large number of weak bonds summing to provide a very strong

adhesion.) Furthermore, if the model is correct, VDW forces should be much more effective than ionic bonding (for instance) at producing spectral changes. On the other hand, if the hypothesis were correct, it would be curious that the stacking of the dye molecules does not also produce such a VDW effect.

At and Above the CMC

At and above the CMC, it is very difficult to draw conclusions about the situation of Methylene Blue with respect to the SDS micelles. There are three possiblities: either Methylene Blue is now *dissolved* in the hydrophobic interior, as in Figure 3-20, or it is charge-complexed with the negative charge coat on the exterior of the micelles, as in Figure 3-21, or it is has been expelled from the micelles and is free in solution. These three models will be called the "dissolution model", the "complexation model", and the "free MB" model.

Comparing Figures 3-17 and 3-11, we can see that the absorption spectrum of MB with SDS above the CMC is very much like that of free MB; the B band has experienced a blueshift very similar to that found in MB in Ethanol. This is consistent with the dissolution model: it exhibits the expected blueshift for a reduction in solvent polarity, as discussed under *Energy Level Structure* in the Methylene Blue section. This data is also consistent with free MB model, if we assume that the presence of the micelles reduces the effective solvent polarity. The

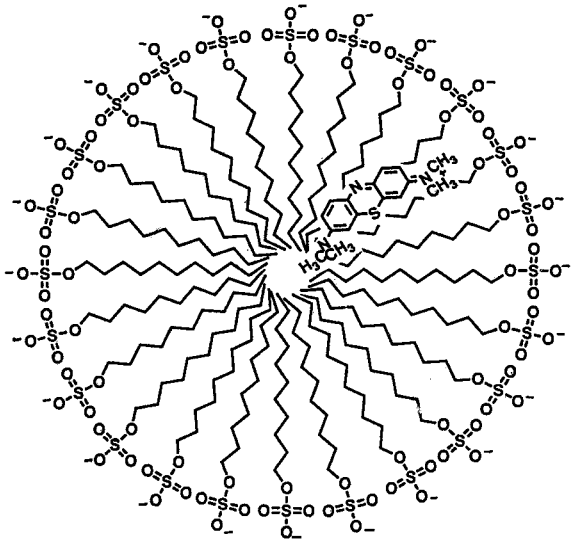

Methylene Blue in Micellar Core

Figure 3-20

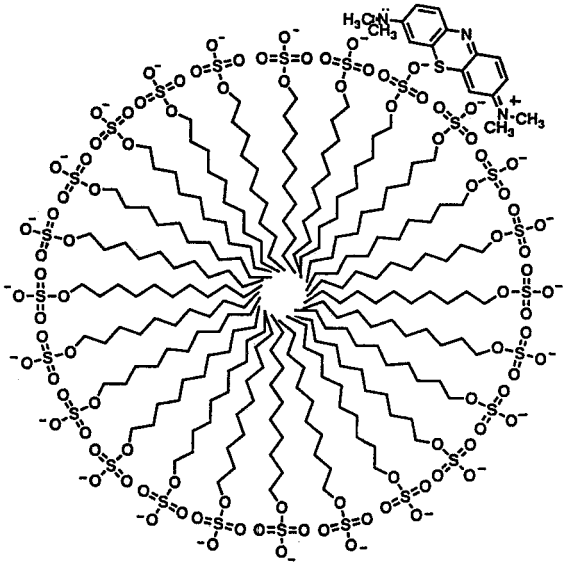

Methylene Blue Charge Complex

Figure 3-21

fluorescence spectrum is also nearly identical to that of free Methylene Blue, experiencing only a slight blue shift in the F-band; since fluorescence spectra of MB in less-polar solvents were not taken, this information cannot be considered to support any of the models. Nor could we obtain fluorescence lifetime information on the F band; the fluorescence lifetime instrument has a long-wavelength limit of 650 nm. NMR data is also unhelpful. In the H-NMR spectrum of 10^{-2} M SDS + 10^{-2} M MB in D_2O (See Figure 3-22), only a small variation of baseline shows at the center of the previously recorded SDS triplet; 2D-HNMR (See Figure 3-23) shows no sign of any SDS peaks! One possible explanation is that the dye was somehow in excess, and enough MB-DS precipitate was formed to remove most of the SDS from solution. (This possibility cannot be checked visually, because the solution is opaque.) In any case, the NMR data does not yield any useful information. Thus, the question of the situation of MB in SDS above the CMC remains open.

CONCLUSION

The interactions of Methylene Blue with itself and with Sodium Dodecyl Sulfate have been studied by visible absorption and fluorescence spectroscopy, with fluorescence lifetime techniques, by HNMR and 2D-HNMR spectroscopy, and by reference to the literature. It has been possible to show with a fairly high level of confidence that Methylene Blue molecules

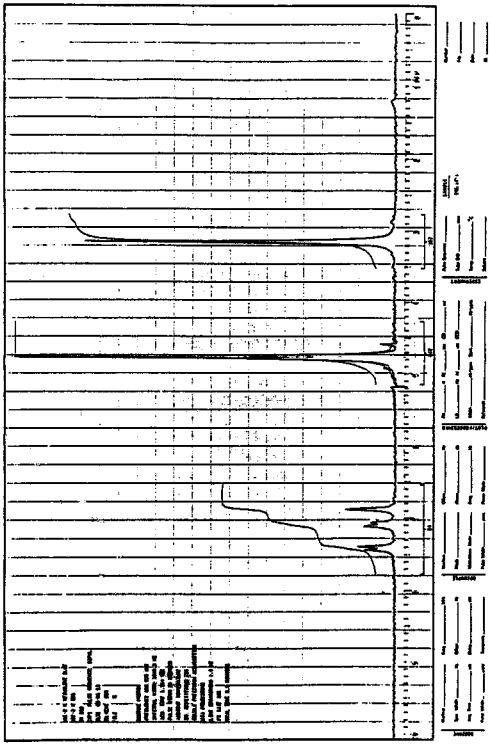

MB + SDS by NMR

Figure 3-22

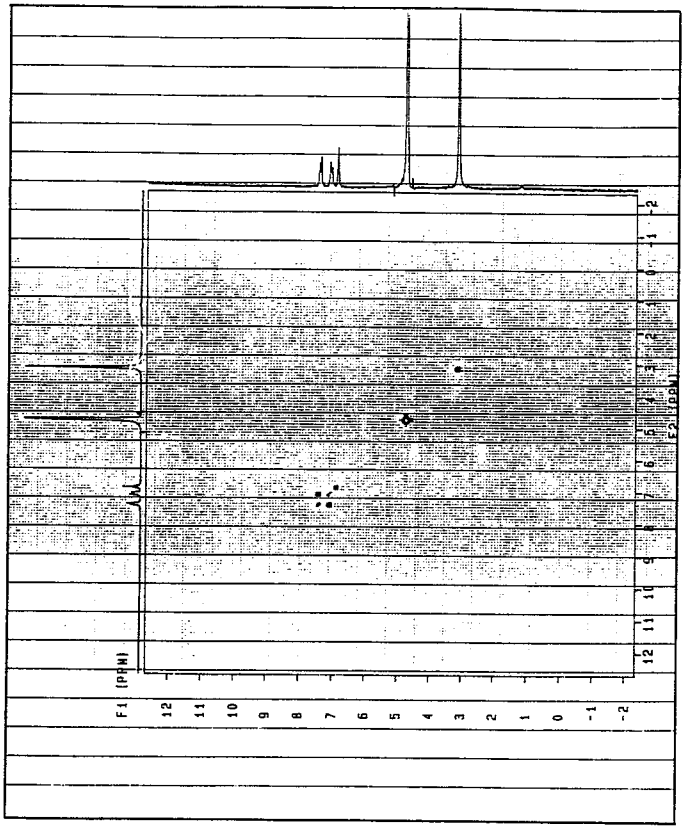

MB + SDS by 2D-HNMR

Figure 3-23

aggregate by stacking in eclipsed conformation. Two effects dominate the interactions between Methylene Blue and Sodium Dodecyl Sulfate below its CMC: the first is the formation of an insoluble MB-DS ion pair. The second is the solvation of this ion pair by 1, 2, or 3 SDS molecules. Hypotheses have been proposed to explain the mechanism of the spectral changes due to dye self-aggregation and aggregation with SDS.

To the best of my knowledge, this is the only investigation of MB self-aggregation and MB-SDS aggregation that has employed fluorescence and fluorescence lifetime techniques. Also, I believe that I am the first to investigate the mechanisms of the spectral changes occuring with these processes.

LITERATURE CITED

1. *CRC Handbook of Analytical Reagents;* Cheng, K.; Ueno, K.; Imamura, T.; CRC Press: Boca Raton, 1990; pp 453-454.

2. Garcia, M. E.; Sanz-Medel, A., *Talanta.* **1986**, *33(3)*, 255-264.

3. Ibid.

4. Ibid.

5. Atherton and Dymond, *J. Phys. Chem.* **1989**, *93*, 6809 - 6813.

6. Baxendale and Rogers, *J. Phys. Chem.* **1982**, *86*, 4906-4909.

7. Skoog, D. *Principles of Instrumental Analysis, 3rd Ed;* CBS College Publishing: New York, 1985; p 186-187.

8. Atkins, P. *Physical Chemistry;* Freeman: New York, 1990; p 503-504.

9. Skoog, D. *Principles of Instrumental Analysis, 3rd Ed;* CBS College Publishing: New York, 1985; p 233.

10. Silverstein, R; Bassler, G; *Spectrometric Identification of Organic Compounds;* Wiley: New York, 1967

11. Skoog, D. *Principles of Instrumental Analysis, 3rd Ed;* CBS College Publishing: New York, 1985; pp 186-187.

12. ibid.

13. Skoog, D. *Principles of Instrumental Analysis, 3rd Ed;* CBS College Publishing: New York, 1985; pp 188-189.

14. Braswell, E, *J. Phys. Chem.* **1984**, *88*, 3653-3658.

15. Tanford, C. *The Hydrophobic Effect;* Wiley: New York, 1973, Introduction.

16. Harris, R. *Nuclear Magnetic Resonance Spectroscopy;* Longman: New York, 1986, pp 144-150.

17. Braswell, E, *J. Phys. Chem.* **1984**, *88*, 3653-3658.

18. Atherton and Dymond, *J. Phys. Chem.* **1989**, *93*, 6809 - 6813.

19. Corrin, M; Klevens, H; Harkins, W. *J. Chem. Phys.* **1946**, *14*, 216.

20. Murkerjee, P.; Mysels, K. *J. Am. Chem. Soc.* **1955**, *77*, 2937.

21. Garcia, M. E.; Sanz-Medel, A., *Talanta.* **1986**, *33(3)*, 255-264.